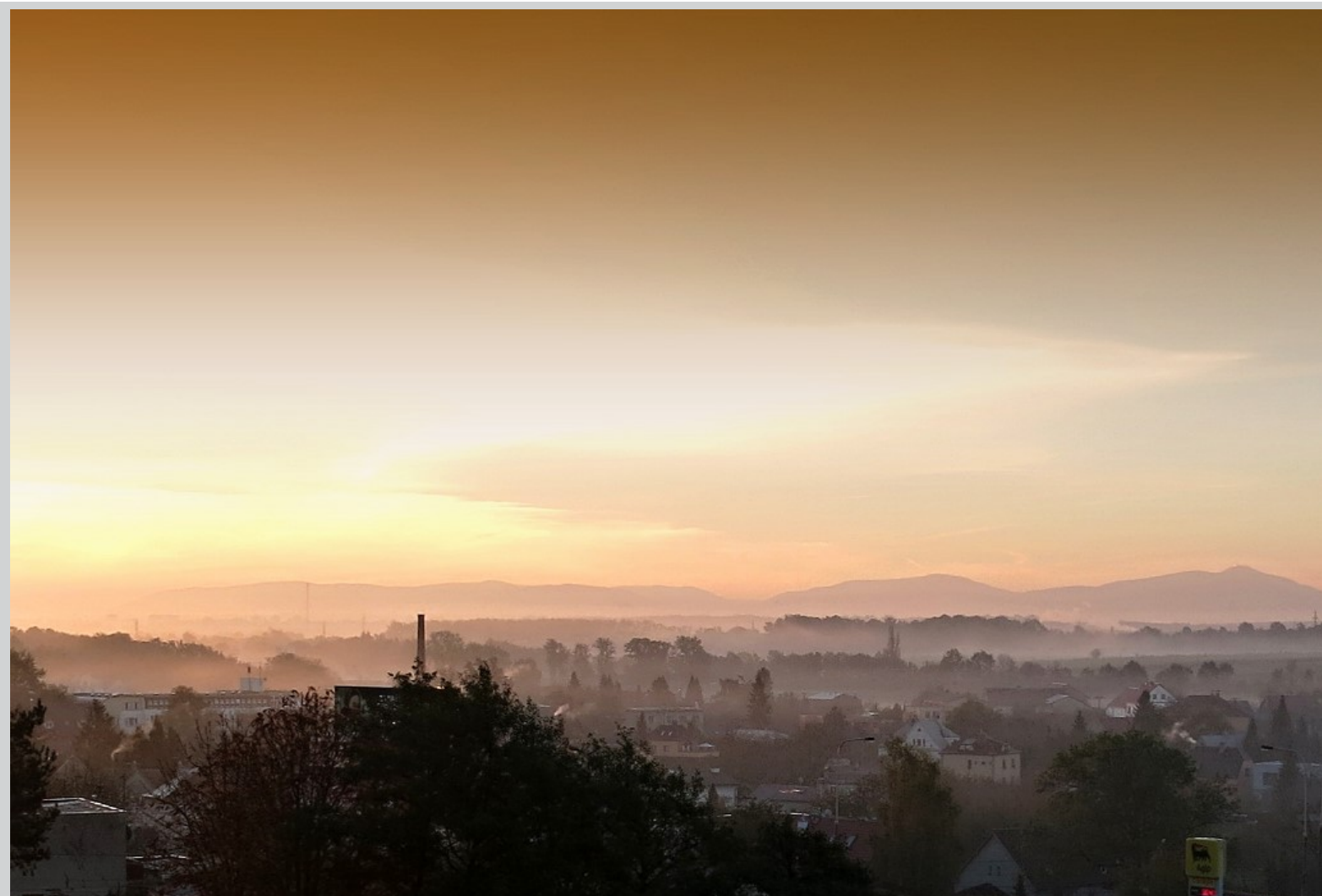


Land cover and traffic data inclusion in PM mapping

December 2018



Authors:

Jan Horálek, Peter de Smet, Philipp Schneider,
Frank de Leeuw, Markéta Schreiberová

ETC/ACM consortium partners: National Institute for Public Health and the Environment (RIVM), Aether, Czech Hydrometeorological Institute (CHMI), Institute of Environmental Assessment and Water Research (CSIC/IDAEA), EMISIA, Institut National de l'Environnement Industriel et des Risques (INERIS), Norwegian Institute for Air Research (NILU), Öko-Institute, Öko-Recherche, Netherlands Environmental Assessment Agency (PBL), Universitat Autònoma de Barcelona (UAB), Umweltbundesamt Wien (UBA-V), Vlaamse Instelling voor Technologisch Onderzoek (VITO), 4sfera Innova

European Environment Agency
European Topic Centre on Air Pollution and
Climate Change Mitigation



Cover photo – Illustration of a city with elevated PM concentrations. © Blanka Krejčí

Legal notice

The contents of this publication do not necessarily reflect the official opinions of the European Commission or other institutions of the European Union. Neither the European Environment Agency, the European Topic Centre on Air Pollution and Climate Change Mitigation nor any person or company acting on behalf of the Agency or the Topic Centre is responsible for the use that may be made of the information contained in this report.

Copyright notice

© European Topic Centre on Air Pollution and Climate Change Mitigation (2018)
Reproduction is authorized provided the source is acknowledged.

More information on the European Union is available on the Internet (<http://europa.eu>).

Authors

Jan Horálek, Markéta Schreiberová: Czech Hydrometeorological Institute (CHMI, CZ)
Peter de Smet, Frank de Leeuw: National Institute for Public Health and the Environment (RIVM, NL)
Philipp Schneider: Norwegian Institute for Air Research (NILU, NO)

European Topic Centre on Air Pollution
and Climate Change Mitigation

PO Box 1
3720 BA Bilthoven
The Netherlands
Tel.: +31 30 274 8562
Fax: +31 30 274 4433
Web: <http://acm.eionet.europa.eu>
Email: etcacm@rivm.nl

Contents

1 Introduction.....	5
2 Methodology	7
2.1 Current methodology	7
2.2 Updated methodology	8
2.3 Uncertainty estimates of the concentration maps	9
3 Input data	11
3.1 Monitoring data.....	11
3.2 Chemical transport modelling data	11
3.3 Altitude, meteorological data, population density	11
3.4 Land cover	12
3.5 Road data.....	13
4 Analysis.....	15
4.1 PM ₁₀	16
4.1.1 Rural and urban background merged concentration maps	16
4.1.2 Traffic map layers	21
4.1.3 Final concentration maps	24
4.1.4 Exposure estimates	28
4.2 PM _{2.5}	33
4.2.1 Rural and urban background merged concentration map.....	33
4.2.2 Traffic map layer inclusion	36
4.2.3 Final concentration map.....	38
4.2.4 Exposure estimates	40
5 Conclusion	43
References.....	45
Annex – On the spatial gradient of NO ₂ and PM along roads	47
A.1 Introduction and Motivation.....	47
A.2 Brief Literature Overview	47
A.3 Results from an experiment using the dispersion model EPISODE	50
A.4 Conclusions	53
References	53

1 Introduction

Annual European-wide air quality maps have been produced using geostatistical techniques for many years (Horálek et al., 2018a and references therein). The mapping method is the *regression – interpolation – merging* mapping, which is based primarily on air quality measurements. It combines monitoring data, chemical transport model outputs and other supplementary data (such as altitude and meteorology) using the linear regression model followed by kriging of its residuals ('residual kriging'), which is applied separately for the rural and urban background areas. The rural and urban background map layers are subsequently merged by population density.

Inclusion of land cover and traffic data demonstrated to improve the quality of the NO₂ map, see Horálek et al. (2017). Currently, this improved methodology is routinely used in the NO₂ mapping ((Horálek et al., 2018a). The improved method adds land cover and road data among the set of the supplementary data. Next to this, urban traffic map layer based on the measurement data from traffic stations is constructed and merged with the rural and urban background map layers in the final merged map. The concluding chapter of Horálek et al. (2017) recommends examining whether a similar approach would improve the maps of other pollutants as well, namely the PM₁₀ and PM_{2.5} maps.

This report follows the mentioned recommendation and examines for PM₁₀ and PM_{2.5} the similar method like has been developed for NO₂. I.e., it examines inclusion of land cover data in the background map layer (and by applying the 1x1 km² resolution in all process steps), as well as the inclusion of the urban traffic layer in the production of the final concentration map and population exposure estimates. The analysis is done based on 2015 data, being the most recent year with all data needed available when this study started.

Chapter 2 describes the methodological aspects. Chapter 3 documents the input data. Chapter 4 presents the analysis and results of the examination of the application of both land cover data and traffic map layer inclusion in the mapping methodology. Chapter 5 discusses the results and summarizes the conclusions.

The Annex presents a brief literature review on the spatial gradients of NO₂ and PM concentrations along the roads. The reason is to compare if the spatial gradients for NO₂ and PM are similar, in order to check whether it is possible to apply in the PM mapping the similar merge of the background and traffic map layers like for NO₂.

2 Methodology

2.1 Current methodology

The mapping methodology used to create the PM₁₀ and PM_{2.5} concentration maps is the so-called *regression – interpolation – merging* mapping as described in Horálek et al. (2018). So far, only background PM₁₀ and PM_{2.5} maps have been constructed, therefore not accounting for traffic, whereas traffic is an important source of PM air pollution.

The mapping method consists of a linear regression model followed by kriging of the residuals from that regression model (residual kriging):

$$\hat{Z}(s_0) = c + a_1 X_1(s_0) + a_2 X_2(s_0) + \dots + a_n X_n(s_0) + \hat{\eta}(s_0), \quad (2.1)$$

where $\hat{Z}(s_0)$ is the estimated concentration at a point s_0 ,
 $X_1(s_0), X_2(s_0), \dots, X_n(s_0)$ are n individual supplementary variables at point s_0 ,
 c, a_1, a_2, \dots, a_n are the $n+1$ parameters of the linear regression model calculated based on the data at the points of measurement,
 $\hat{\eta}(s_0)$ is the spatial interpolation of the residuals of the linear regression model at point s_0 , based on the residuals at the points of measurement.

The spatial interpolation of the regression's residuals is carried out using ordinary kriging, according to

$$\hat{\eta}(s_0) = \sum_{i=1}^N \lambda_i \eta(s_i) \quad \text{with} \quad \sum_{i=1}^N \lambda_i = 1, \quad (2.2)$$

where $\hat{\eta}(s_0)$ is the interpolated value at a point s_0 , derived from the residuals of the linear regression model at the points of measurement $s_i, i = 1, \dots, N$,
 $\eta(s_i)$ are the residuals of the linear regression model at N points of measurement $s_i, i = 1, \dots, N$,
 $\lambda_1, \dots, \lambda_N$ are the estimated weights based on the variogram, see Cressie (1993).

Prior to linear regression and interpolation, a logarithmic transformation to measurements and EMEP model concentrations¹ has been executed as that contributes to an improved fit of the regression model. After interpolation, a back-transformation is applied.

Separate map layers are created for the rural and the urban background areas on a grid at 10x10 km² resolution. The rural background map layer is based on the rural background stations and the urban background map layer on the urban and the suburban background stations. Subsequently, the rural background map layer and the urban background map layer are merged into one combined final map using a weighting procedure based on the population density grid at 1x1 km² resolution, according to

$$\hat{Z}_F(s_0) = (1 - w_U(s_0)) \cdot \hat{Z}_R(s_0) + w_U(s_0) \cdot \hat{Z}_{UB}(s_0) \quad (2.3)$$

where $\hat{Z}_F(s_0)$ is the resulting estimated concentration in a grid cell s_0 for the final map,
 $\hat{Z}_{UB}(s_0)$ is the estimated concentration in a grid cell s_0 for the urban background map layer,
 $\hat{Z}_R(s_0)$ is the estimated concentration in a grid cell s_0 for the rural background map layer,

¹ The results of the EMEP model (Simpson et al, 2012) is one of the supplementary variables used in equation (2.1), see also section 3.2.

$w_U(s_0)$ is the weight representing the ratio of the urban character of the grid cell s_0 .

The weight $w_U(s_0)$ is calculated according to

$$\begin{aligned} w_U(s_0) &= 0 && \text{for } p(s_0) \leq 100 \\ &= \frac{p(s_0)-100}{400} && \text{for } 100 < p(s_0) < 500 \\ &= 1 && \text{for } p(s_0) > 500 \end{aligned} \quad (2.4)$$

where $p(s_0)$ is the population in the i -th grid cell s_0 .

In the case of PM_{2.5} mapping, the PM_{2.5} measurement data are supplemented with the data from so-called pseudo PM_{2.5} stations. These pseudo PM_{2.5} station data are the estimates of PM_{2.5} concentrations at PM₁₀ measurement stations where no PM_{2.5} concentrations are measured. These estimates are based on the multiple linear regression of PM_{2.5} concentrations (dependent variable) and PM₁₀ concentrations enriched with different supplementary data (independent variables), obtained from stations where both pollutants are measured. In this regression, all background stations (both rural and urban/suburban) are handled together without distinction on type. For further details, see Horálek et al. (2007, 2018).

Population exposure for individual countries and for Europe as a whole is calculated from the air quality maps and population density data, both at 1x1 km² resolution. For each concentration class ' j ', the percentage population per country as well as the European-wide total is determined:

$$P_j = \frac{\sum_{i=1}^N I_{ij} P_i}{\sum_{i=1}^N P_i} \cdot 100 \quad (2.5)$$

where P_j is the percentage population living in areas of the j -th concentration class in either the country or in Europe as a whole,
 p_i is the population in the i -th grid cell,
 I_{ij} is the Boolean 0-1 indicator showing whether the concentration in the i -th grid cell is within the j -th concentration class ($I_{ij} = 1$), or not ($I_{ij} = 0$),
 N is the number of grid cells in the country or in Europe as a whole.

In addition, we express per-country and European-wide exposure as the population-weighted concentration, i.e. the average concentration weighted according to the population in a grid cell:

$$\hat{c} = \frac{\sum_{i=1}^N c_i P_i}{\sum_{i=1}^N P_i} \quad (2.6)$$

where \hat{c} is the population-weighted average concentration in the country or in Europe as a whole,
 c_i is the concentration in the i -th grid cell.

2.2 Updated methodology

For both rural and urban background map layers, the use of an advanced set of the supplementary variables is examined. The supplementary variables of Equation 2.1 are selected from a large set of

variables, now including land cover and road data variables as well, through a stepwise regression and backwards elimination of the weakest performing variables (Horálek et al., 2007). In this selection two criteria are applied in general, similar to Beelen et al. (2009): a variable is not excluded from the regression model that (i) increases the adjusted R² value by more than 1%, and (ii) has a coefficient that conforms to the pre-specified direction of association between the variable and the pollutant. Contrary to the current methodology of Section 2.1, the separate rural and urban background map layers are constructed in 1x1 km² resolution.

Next to this, an additional map of the traffic related air quality, the so-called *traffic map layer*, is constructed based on the urban traffic stations according to Equation 2.1, similar to the NO₂ mapping (Horálek et al., 2017, 2018). As the traffic map layer is representative for urban traffic areas only, we include it in the final map using a weighting procedure as extension on the urban parameters of Eq.2.3, such that we attain Eq.2.7

$$\hat{Z}_F(s_0) = (1 - w_U(s_0)) \cdot \hat{Z}_R(s_0) + w_U(s_0)(1 - w_T(s_0)) \cdot \hat{Z}_{UB}(s_0) + w_U(s_0)w_T(s_0) \cdot \hat{Z}_T(s_0) \quad (2.7)$$

where $\hat{Z}_T(s_0)$ is the estimated concentration in a grid cell s_0 for the urban traffic map layer,

$w_T(s_0)$ is the weight representing ratio of areas exposed to traffic air quality in a grid cell s_0 .

The weight $w_T(s_0)$ is based on the buffers around the roads further detailed at Section 3.5. The setting of the weight is discussed later in this paper (Sections 4.1.3 and 4.2.3).

The population exposure percentage using the traffic map layer is calculated according to

$$P_j = \frac{\sum_{i=1}^N I_{Bij}(1 - w_U(i)w_T(i))p_i + \sum_{i=1}^N I_{Tij}w_U(i)w_T(i)p_i}{\sum_{i=1}^N p_i} \cdot 100 \quad (2.8)$$

where I_{Bij} is the Boolean 0-1 indicator showing whether the background air quality concentration (estimated by the combined rural/urban background map layer) in the i -th grid cell is within the j -th concentration class ($I_{Bij} = 1$), or not ($I_{Bij} = 0$),

I_{Tij} is the Boolean 0-1 indicator showing whether the traffic air quality concentration in the i -th grid cell is within the j -th concentration class ($I_{Tij} = 1$), or not ($I_{Tij} = 0$).

The population-weighted concentration is calculated according to the Equation 2.6, where population exposure c_i is calculated according to

$$\begin{aligned} c_i = \hat{Z}_F(i) &= (1 - w_U(i)) \cdot \hat{Z}_R(i) + w_U(i) \cdot \hat{Z}_U(i) \\ &= (1 - w_U(i)) \cdot \hat{Z}_R(i) + w_U(i)(1 - w_T(i)) \cdot \hat{Z}_{UB}(i) + w_U(i)w_T(i) \cdot \hat{Z}_T(i) \end{aligned} \quad (2.9)$$

Comparing Equations 2.3 and 2.9, one can see that no separate calculations for the background and the traffic map layers are needed. The reason is in the use of the population in 1x1 km² grid resolution.

2.3 Uncertainty estimates of the concentration maps

The uncertainty estimation of the mapping results is based on the 'leave one out' *cross-validation* method (Horálek et al., 2007, 2018). It computes the spatial interpolation for each measurement point based on all available information except from this point. The results of the cross-validation are compared with the

measurement data using statistical indicators and scatter plots. The main indicators used are *root mean squared error (RMSE)* and *bias*:

$$RMSE = \sqrt{\frac{1}{N} \sum_{i=1}^N (\hat{Z}(s_i) - Z(s_i))^2} \quad Bias = \frac{1}{N} \sum_{i=1}^N (\hat{Z}(s_i) - Z(s_i)) \quad (2.10)$$

where $Z(s_i)$ is the observed air quality indicator value at the i^{th} point,
 $\hat{Z}(s_i)$ is the estimated air quality indicator value at the i^{th} point using other information, except the observed indicator value at the i^{th} point,
 N is the number of the observational points.

Next to the RMSE expressed in absolute units, one could express this uncertainty in percentage by relating the RMSE to the mean of the air quality indicator value for all stations:

$$RRMSE = \frac{RMSE}{\frac{1}{N} \sum_{i=1}^N Z(s_i)} \cdot 100 \quad (2.11)$$

where $RRMSE$ is the relative RMSE, expressed as percentage.

Other cross-validation indicators are the coefficient of determination R^2 and the regression equation parameters *slope* and *intercept*, following from the scatter plot between the cross-validation predicted and the observed concentrations.

Next to the cross-validation, in some cases also the simple *comparison of measured concentration and predicted grid values of the grid in which the station is located* was done. In these cases, the similar statistical indicators as in cross-validation are used (i.e. $RMSE$, *bias*, R^2 , *slope* and *intercept*).

3 Input data

3.1 Monitoring data

Air quality station monitoring data for the relevant year are extracted from the EEA Air Quality e-Reporting database, EEA (2017a). This data set is supplemented with several EMEP stations from the EBAS database (NILU, 2017) and with several others presented in CHMI (2017). For details, see Horálek et al. (2018). Only data from stations classified by the Air Quality e-Reporting database and/or EBAS of the type *background* and *traffic* for the areas *rural*, *suburban* and *urban* are used. Station type *industrial* is not considered; it represents local scale concentration levels not applicable at the mapping resolution employed. The following pollutants and their indicators are considered:

- PM₁₀ – annual average [$\mu\text{g}\cdot\text{m}^{-3}$], year 2015
- 90.4 percentile of daily means [$\mu\text{g}\cdot\text{m}^{-3}$], year 2015
- PM_{2.5} – annual average [$\mu\text{g}\cdot\text{m}^{-3}$], year 2015

Only stations with annual data coverage of at least 75 percent are used. We excluded the stations outside the EEA map extent *Map_1c* (EEA, 2011). This map extent is used at the maps presented in this paper.

In total, 348 rural background stations, 1102 urban/suburban background stations and 596 urban/suburban traffic stations are used for PM₁₀. While for PM_{2.5} we used 167 rural background stations, 543 urban/suburban background stations and 246 urban/suburban traffic stations. Due to the small number of the rural traffic stations (i.e. 9 resp. 4), these stations are further not considered and only the estimation of the urban traffic related air quality is discussed in this paper (see Sections 4.1.2 and 4.2.2).

3.2 Chemical transport modelling data

The chemical dispersion model used in this paper is the EMEP MSC-W (formerly called Unified EMEP) model (version rv4.15), which is an Eulerian model. Simpson et al. (2012) and https://wiki.met.no/emep/page1/emepmscw_opensource (web site of Norwegian Meteorological Institute) describe the model in more detail. Emissions for the relevant year 2015 (Mareckova et al., 2017) are used and the model is driven by ECMWF meteorology for the relevant year 2015. EMEP (2017) provides details on the EMEP modelling for 2015. The resolution of this model run is $0.1^\circ \times 0.1^\circ$, i.e. circa $10 \times 10 \text{ km}^2$. Information from this model has been converted to $1 \times 1 \text{ km}^2$ grid resolution: the data representing the EMEP grid cells are imported into *ArcGIS* and transformed into the ETRS89-LAEA5210 projection, subsequently converted into a $100 \times 100 \text{ m}$ resolution raster grid and spatially aggregated into the reference EEA $1 \times 1 \text{ km}^2$ grid. The parameters used are the same as for the monitoring data, i.e.

- PM₁₀ – annual average [$\mu\text{g}\cdot\text{m}^{-3}$], year 2015
- 90.4 percentile of daily means [$\mu\text{g}\cdot\text{m}^{-3}$], year 2015
- PM_{2.5} – annual average [$\mu\text{g}\cdot\text{m}^{-3}$], year 2015

3.3 Altitude, meteorological data, population density

The *altitude* data field (in m) with an original grid resolution of 15×15 arc-seconds comes from U.S. Geological Survey Earth Resources Observation and Science (GTOPO), see Danielson et al. (2011). The data were converted into the ETRS89-LAEA5210 projection, resampled to $100 \times 100 \text{ m}$ resolution, shifted to the extent of EEA reference grid, and spatially aggregated into $1 \times 1 \text{ km}^2$ grid resolution. Next to this, another aggregation has been executed based on the $1 \times 1 \text{ km}^2$ grid cells, i.e. the floating averaging of the circle with *radius of 5 km* around all relevant grid cells. For motivation, see Section 3.4.

The *meteorological parameters* used are *wind speed* (annual average for 2015, in $m.s^{-1}$), *surface net solar radiation* (annual average of daily sum for 2015, $MWs.m^{-2}$), *temperature* (annual average for 2015, °C) and *relative humidity* (annual average for 2015, percentage). The daily data in resolution 15x15 arc-seconds were extracted from the Meteorological Archival and Retrieval System (MARS) of ECMWF, see ECMWF (2017). For details, see Horálek et al. (2007). The data have been imported into ArcGIS as a point shapefile. Each point represents the centre of a grid cell. The shapefile has been converted into ETRS89-LAEA5210 projection, converted into a 100x100 m resolution raster grid and spatially aggregated into the reference EEA 1x1 km^2 grid.

Population density (in inhabitants. km^{-2} , census 2011) is based on Geostat 2011 grid dataset (Eurostat, 2014). The dataset is in 1x1 km^2 resolution, in the EEA reference grid. For regions not included in the Geostat 2011 dataset we use as alternative sources JRC (2009) and ORNL (2008) data. For details, see Horálek et al. (2018). Next to the basic resolution of 1x1 km^2 , the floating averaging of the circle with radius 5 km around all individual 1x1 km^2 grid cells has been prepared. For motivation, see Section 3.4.

3.4 Land cover

CORINE Land Cover 2006 – grid 100 x 100 m^2 , Version 18.5 (09/2016) is used (EEA, 2016b). The country missing in this database is Andorra; the areas missing are Faroe Islands and Jan Mayen.

In order to reduce the high number of degrees of freedom in the CORINE Land Cover description, the 44 CLC classes (<http://www.eea.europa.eu/data-and-maps/data/clc-2006-vector-data-version-3/corine-land-cover-2006-classes>) have been re-grouped into the 8 more general classes in agreement with the recommendations of Horálek et al. (2017), i.e. similarly like in Beelen et al. (2013).

Table 0.1 Definition of general land cover classes, based on CLC2006 classes

Label	General class description	CLC classes grid codes	CLC classes codes	CLC classes description
HDR	High density residential areas	1	111	Continuous urban fabric
LDR	Low density residential areas	2	112	Discontinuous urban fabric
IND	Industry	3, 7 – 9	121, 131 – 133	Industrial or commercial units, Mineral extraction sites, Dump sites, Construction sites
TRAF	Traffic	4 – 6	122 – 124	Road and rail networks and associated land, Ports, Airports
UGR	Urban green	10 – 11	141 – 142	Artificial, non-agricultural vegetated areas
AGR	Agricultural areas	12 – 22	211 – 244	Agricultural areas
NAT	Natural areas	23 – 34	311 – 335	Forest and semi natural areas
OTH	Other areas	35 – 44	411 – 523	Wetlands, Water bodies

Like in Horálek et al. (2017), two aggregations are used, i.e. into 1x1 km^2 grid and into the circle with radius of 5 km, as a floating average for all 1x1 km^2 grid cells. The reason for these two aggregations is this: 1x1 km^2 is directly related to the mapping and calculation resolution, the circle with radius of 5 km corresponds to a buffer of 5 km often used in LUR models (Hoek et al., 2008). For each general CLC class we spatially aggregated the high land use resolution into the 1x1 km^2 EEA standard grid resolution. The aggregated grid square value represents for each general class the total area of this class as percentage of the total 1x1 km^2 square area. For the floating averaging of the circle with radius 5 km around all relevant 1x1 km^2 grid cells, the aggregated grid square value represents for each general class the total area of this class as percentage of the total area of this circle (which is 81 square kilometers; this value is influenced by the 1x1 km^2 resolution of the aggregated land cover data).

In the analysis, the first seven classes have been used only, while the class OTH has been omitted as redundant, as it can be expressed by the other general classes: the percentage of the grid square area attributed to this class can be calculated by subtracting the percentages attributed to other seven classes from 100.

3.5 Road data

GRIP vector road type data base provided by PBL is used (PBL, 2018). For description, see Meijer et al. (2018). In this data base, road types are distributed into five classes, from highways to local roads and streets. In agreement with the conclusion of Horálek et al. (2017), classes 1 (Highways, coded T1), 2 (Primary roads, T2) and 3 (Secondary roads, T3) are used. Based on the GRIP vector data, *ratio of the area influenced by traffic* represented by buffers around the roads were calculated in ESRI ArcGIS for individual road type classes 1 – 3 and for their combination (i.e. for classes 1 – 3 together), at all 1x1 km² grid cells. A buffer of 75 metres distance at each side from each road vector is taken for the roads of classes 1 (coded T1_buffer75m) and 2 (T2_buffer75m), while a buffer of 50 meters is taken for the roads of class 3 (T3_buffer50m). For motivation, see Horálek et al. (2017).

4 Analysis

In this section we present the analysis in which the potential improvement of PM₁₀ and PM_{2.5} mapping is examined. In the case of PM₁₀, the analysis is done for both annual average and 90.4 percentile. For PM_{2.5}, only the annual average is used. Thus, all three routinely mapped PM indicators are handled.

At first, we examine potential improvement of the PM mapping by including land cover and road data in the rural and urban background mapping, going to 1x1 km² resolution. Then, we test the creation of the urban traffic map layer using measurement data from the urban traffic stations and available supplementary data, for further inclusion in the final map. Next to the final maps, also exposure estimates are prepared.

For all map layers, i.e. rural background, urban background, and urban traffic, the set of supplementary parameter data are tested on their suitability for inclusion in the linear regression model and includes 27 variables. Note that all variables are in a 1x1 km² default mapping resolution. The set consists of:

- EMEP model output
- Altitude: - 1x1 km² grid altitude
 - Floating average of circle radius 5 km around 1x1 km² grid cell
- Meteorological parameters: - Wind speed
 - Temperature
 - Surface net solar radiation
 - Relative humidity
- Population density: - 1x1 km² grid
 - Circle radius 5 km around 1x1 km² grid cell
- Land cover type (as percentage of 1x1 km² grid and of radius 5 km):
 - HDR (coded *HDR_1km* and *HDR_5km_r*)
 - LDR (coded *LDR_1km* and *LDR_5km_r*)
 - IND (coded *IND_1km* and *IND_5km_r*)
 - TRAF (coded *TRAF_1km* and *TRAF_5km_r*)
 - UGR (coded *UGR_1km* and *UGR_5km_r*)
 - AGR (coded *AGR_1km* and *AGR_5km_r*)
 - NAT (coded *NAT_1km* and *NAT_5km_r*)
- Road data: - Area influenced by traffic for road type class 1 (coded *T1_buffer75m*)
 - Area influenced by traffic for road type class 2 (coded *T2_buffer75m*)
 - Area influenced by traffic for road type class 3 (coded *T3_buffer50m*)
 - Area influenced by traffic for road type classes 1–3 together (coded *T123_buffer*)

In all cases, the most useful supplementary data are selected through a stepwise regression and backwards elimination as described in Section 2.2. For different pollutants and area types, different sets of supplementary variables are selected for inclusion in the linear regression calculation model. For all pollutants and area types, several variants of sets of supplementary variables are examined and mutually compared. Details are given in the next sections.

In Section 4.1, we present the analysis for PM₁₀. Section 4.2 presents the analysis for PM_{2.5}. The analysis is based on 2015 data, being the most recent year with all data needed available when this study started.

4.1 PM₁₀

4.1.1 Rural and urban background merged concentration maps

For both rural and urban background map layers, we have examined the improvement that the inclusion of the land cover and road type data may provide in the mapping process. We have compared the mapping variants without and with the inclusion of land cover and road type data.

As basic variant, we have used the current methodology (Horálek et al., 2018a), labelled as (C), which is performed for the separate rural and urban background layers at a 10x10 km² grid resolution (while a 1x1 km² resolution is applied in the final merge of these map layers). For better comparability with the improved variant including the land cover (see below) that is executed on a 1x1 km² grid resolution in all mapping process steps, we introduce also the so called 'like current' variant, labelled as (C1). In this (C1) variant, exactly the same set of supplementary variables as at variant (C) is applied (i.e. EMEP model output, altitude and wind speed in rural areas, and EMEP model output in the urban background areas), but contrary to (C) variant, (C1) is executed on a 1x1 km² grid resolution in all mapping process steps.

The basic variants (C and C1) have been compared with a variant including the land cover data, labelled as (L). Additionally, we have examined also this variant including the land cover data, but now without the logarithmic transformation normally applied in PM mapping (see Horálek et al., 2010, 2018); we label this variant as (L0). The reason for including this variant (L0) is to verify whether the logarithmic transformation improves the PM₁₀ mapping results even though the additional supplementary data are included.

To explore in depth the level of improvement of the application of land cover data itself on the PM₁₀ mapping at variant (L), we introduced a variant 'without the inclusion of land cover data'. In this variant, the selection procedure as described in Section 2.2 was applied for the whole set of supplementary variables apart from land cover parameters. We labelled that variant as (N). The reason for examining this (N) variant is this: if we had inter-compared only the (L) and (C) resp. (C1) variants, one could object that another supplementary parameter in the 1x1 km² resolution could also improve the fit, without the use of the land cover data. The additional benefit is that it allows for the selection of the optimal variant for the areas with the lack of the land cover data.

The most useful supplementary data in (N), (L) and (L0) variants have been selected through a stepwise regression and backwards elimination (Section 2.2), for both rural and urban background areas. Table 4.1 provides the overview of all the mutually compared variants, including their specific set of used supplementary data in terms of several classes of variables, as described in the introductory section of Chapter 4. The road data are handled together with the land cover data in a column labelled as "land cover".

Table 4.1 List of mutually compared variants of the PM₁₀ mapping method, rural and urban background areas

Lab.	Variant Description	Area type	Grid resolution	Model EMEP	Alt.	Meteo	Popul. density	Land cover
(C)	Current, 10x10 km	Rural background	10x10 km ²	+	+	+	-	-
		Urban background	10x10 km ²	+	-	-	-	-
(C1)	Like current, 1x1 km	Rural background	1x1 km ²	+	+	+	-	-
		Urban background	1x1 km ²	+	-	-	-	-
(L)	Land cover included	Rural background	1x1 km ²	+	+	+	- (a)	+
		Urban background	1x1 km ²	+	- (a)	+	+	+
(L0)	Land cover included, without lognormal transposition	Rural background	1x1 km ²	+	+	+	- (a)	+
		Urban background	1x1 km ²	+	- (a)	+	+	+
(N)	Without land cover	Rural background	1x1 km ²	+	+	+	- (a)	-
		Urban background	1x1 km ²	+	- (a)	+	- (a)	-

(a) Excluded in the backward stepwise selecting procedure

Table 4.2 presents the supplementary variables ultimately selected and applied, including their relevant statistical performance parameters at both the multiple linear regression and the subsequent interpolation by ordinary kriging of its residuals, for the PM₁₀ annual average. Table 4.3 shows the similar parameters for the PM₁₀ indicator 90.4 percentile of daily means.

For the variant including land cover (L), the selected variables are EMEP model output, altitude, wind speed, relative humidity, and the land cover parameter NAT_1km in the rural areas and EMEP model output, wind speed, population density, and land cover parameter AGR_5km_r in the urban background areas, for the annual average. For the 90.4 percentile of daily means, the same variables like for the annual average are selected in the rural areas, while in the urban background areas relative humidity and temperature are selected instead of wind speed. It can be seen that quite surprisingly, no road data are among selected variables.

Table 4.2 Parameters of the linear regression models and of the ordinary kriging (nugget, sill, range) of PM₁₀ annual average for 2015 in rural background, urban background and urban traffic areas for different mapping variants

Linear Regr. Model + OK of residuals	(C) Current 10x10		(C1) Like current 1x1		(L) LC included		(L0) LC incl., no log. tr.		(N) Without LC	
	rural coeff.	urb. b. coeff.	rural coeff.	urb. b. coeff.	rural coeff.	u. b. coeff.	rural coeff.	u. b. coeff.	rural coeff.	urb. b. coeff.
c (constant)	1.87	2.28	1.95	2.28	6.85	2.36	83.65	147.58	6.53	2.57
a1 (EMEP model)	0.565	0.323	0.532	0.320	0.494	0.283	0.516	0.405	0.520	0.295
a2 (altit_1km)	-0.0004		-0.0005		-0.0004		-0.0058		-0.0005	
a2 (altit_5km_r)										
a3 (wind speed)	-0.101		-0.097		-0.059	-0.050	-1.173		-0.066	-0.061
a4 (rel. humidity)					-0.053		-0.709	-1.379	-0.050	
a5 (temperature)								-0.509		
a6 (population d.)						0.012		0.234		
a7 (NAT_1km)					-0.0019		-0.0328			
a8 (AGR_5km_r)						0.0035		0.0878		
Adjusted R²	0.58	0.13	0.62	0.13	0.67	0.23	0.60	0.19	0.64	0.16
St. Err. [µg.m⁻³]	0.248	0.298	0.238	0.298	0.221	0.280	3.77	7.33	0.229	0.292
Nugget	0.035	0.023	0.024	0.025	0.018	0.029	7	23	0.021	0.024
Sill	0.063	0.083	0.054	0.081	0.046	0.074	14	51	0.049	0.081
Range [km]	1000	1000	1000	1000	1000	1000	1000	1000	1000	1000

Note: Dark grey indicates variables not considered in the variant of the linear regression model. Light grey indicates variables not selected in the variant by the selecting procedure.

Table 4.3 Parameters of the linear regression models and of the ordinary kriging (nugget, sill, range) of PM₁₀ indicator 90.4 percentile of daily means for 2015 in rural background, urban background and urban traffic areas for different mapping variants

Linear Regr. Model + OK of residuals	(C) Current 10x10		(C1) Like current 1x1		(L) LC included		(L0) LC incl., no log. tr.		(N) Without LC	
	rural	urb. b.	rural	urb. b.	rural	u. b.	rural	u. b.	rural	urb. b.
	coeff.	coeff.	coeff.	coeff.	coeff.	coeff.	coeff.	coeff.	coeff.	coeff.
c (constant)	2.11	2.62	2.19	2.63	5.26	8.45	116.75	283.45	4.89	9.78
a1 (EMEP model)	0.528	0.326	0.501	0.322	0.465	0.333	0.340	0.355	0.484	0.333
a2 (altitude_1km)	-0.0004		-0.0004		-0.0003		-0.0105		-0.0004	
a3 (altit._5km_r)										
a4 (wind speed)	-0.086		-0.081		-0.056		-2.287	-2.623	-0.064	
a5 (rel. humidity)					-0.032	-0.061	-0.875	-1.440	-0.029	-0.073
a6 (temperature)						-0.033		0.460		-0.029
a7 (population d.)						0.011				
a8 (NAT_1km)					-0.0020		-0.0639			
a9 (AGR_5km_r)						0.0044		0.1904		
Adjusted R²	0.54	0.11	0.55	0.11	0.59	0.25	0.52	0.18	0.56	0.18
St. Err. [µg.m⁻³]	0.261	0.344	0.256	0.344	0.244	0.317	7.80	16.17	0.253	0.331
Nugget	0.028	0.023	0.022	0.025	0.017	0.029	26	112	0.019	0.022
Sill	0.068	0.097	0.060	0.113	0.054	0.090	60	251	0.058	0.110
Range [km]	1000	740	1000	1000	1000	790	1000	1000	1000	1000

Note: Dark grey indicates variables not considered in the variant of the linear regression model. Light grey indicates variables not selected in the variant by the selecting procedure.

Comparison by cross-validation

Table 4.4 presents the mapping results of all variants for PM₁₀ annual average, with their different sets of supplementary data that are mutually compared by means of the 'leave one out' cross-validation (Section 2.3), separate for the rural background and urban background areas. Table 4.5 presents the similar table for PM₁₀ indicator 90.4 percentile. The tables present the statistics of each combination of variant and type of area and provide the level of best performance by including a colour ranking: the darker the green marking, the better performance.

Table 4.4 Comparison of different method variants of spatial interpolation showing RMSE, RRMSE, bias, R² and linear regression from the cross-validation scatter plots for PM₁₀ annual mean in rural background (top) and urban background (bottom) areas, 2015. Units: µg.m⁻³ except RRMSE and R².

Spatial interpolation variant + supplementary data used		Rural background areas				
		RMSE	RRMSE	Bias	R ²	Regr. eq.
(C)	Current, 10x10 km ² (EMEP, altitude, wind speed)	3.2	19.4%	0.1	0.711	y = 0.729x + 4.6
(C1)	Like current, 1x1 km ² (EMEP, altitude, wind speed)	3.0	18.2%	0.0	0.746	y = 0.748x + 4.2
(L)	Land cover included, 1x1 km ² (EMEP, altitude, w. sp., rel. hum., LC)	2.9	17.3%	0.0	0.771	y = 0.788x + 3.5
(L0)	LC included, no log. trans., 1x1 km ² (EMEP, alt., w. sp., rel. hum. LC)	3.1	18.4%	0.0	0.740	y = 0.735x + 4.4
(N)	Without LC, 1x1 km ² (EMEP, altitude, wind sp., rel. hum.)	3.0	18.2%	0.0	0.747	y = 0.767x + 3.9
Spatial interpolation variant + supplementary data used		Urban background areas				
		RMSE	RRMSE	Bias	R ²	Regr. eq.
(C)	Current, 10x10 km ² (EMEP)	4.5	19.2%	0.0	0.689	y = 0.691x + 7.3
(C1)	Like current, 1x1 km ² (EMEP)	4.7	19.8%	0.0	0.670	y = 0.673x + 7.8
(L)	Land cover included, 1x1 km ² (EMEP, wind speed, pop. d., LC)	4.9	20.8%	0.1	0.638	y = 0.680x + 7.7
(L0)	LC included, no log. trans., 1x1 km ² (EMEP, rel. hum., temp., pop. d, LC)	4.9	20.7%	0.0	0.640	y = 0.679x + 7.6
(N)	Without LC, 1x1 km ² (EMEP, wind speed)	4.7	20.1%	0.0	0.661	y = 0.679x + 7.6

Table 4.5 Comparison of different method variants of spatial interpolation showing RMSE, RRMSE, bias, R² and linear regression from the cross-validation scatter plots for PM₁₀ indicator 90.4 percentile of daily means in rural background (top) and urban background (bottom) areas, 2015. Units: µg.m⁻³ except RRMSE and R².

Spatial interpolation variant + supplementary data used		Rural background areas				
		RMSE	RRMSE	Bias	R ²	Regr. eq.
(C)	Current, 10x10 km ² (EMEP, altitude, wind speed)	6.2	21.1%	0.1	0.701	y = 0.744x + 7.6
(C1)	Like current, 1x1 km ² (EMEP, altitude, wind speed)	5.9	20.3%	0.0	0.723	y = 0.752x + 7.3
(L)	Land cover included, 1x1 km ² (EMEP, alt., w. sp., rel. hum., LC)	5.6	19.1%	0.0	0.754	y = 0.781x + 6.4
(L0)	LC included, no log. trans., 1x1 km ² (EMEP, alt., w. sp., rel. hum., LC)	6.1	21.0%	0.1	0.703	y = 0.718x + 8.3
(N)	Without LC, 1x1 km ² (EMEP, altitude, wind sp., rel. hum.)	5.8	20.0%	0.0	0.730	y = 0.756x + 7.1
Spatial interpolation variant + supplementary data used		Urban background areas				
		RMSE	RRMSE	Bias	R ²	Regr. eq.
(C)	Current, 10x10 km ² (EMEP)	10.8	25.6%	-0.1	0.635	y = 0.638x + 15.3
(C1)	Like current, 1x1 km ² (EMEP)	10.8	25.7%	-0.1	0.632	y = 0.635x + 15.3
(L)	Land cover included, 1x1 km ² (EMEP, rel. hum., temp., pop. d., LC)	11.3	26.9%	0.2	0.602	y = 0.647x + 15.0
(L0)	LC included, no log. trans., 1x1 km ² (EM., rel. hum., temp., w. sp., LC)	11.2	26.8%	0.0	0.604	y = 0.642x + 15.1
(N)	Without LC, 1x1 km ² (EMEP, rel. hum., temperature)	10.9	26.0%	-0.1	0.625	y = 0.638x + 15.1

It can be seen that the best results in the rural background areas are given by the variant (L), i.e. including land cover at both PM₁₀ indicators. This variant uses EMEP model, altitude, wind speed, relative humidity and land cover class of natural areas as supplementary variables. Compared to the current methodology (C), one can see the improvement of the relative RMSE (RRMSE) from 19 % to 17 % for the annual average and from 21 % to 19 % for the 90.4 percentile. A comparison of (C), (C1) and (L) indicates that this improvement is partly related to the higher resolution of (L) compared to (C). The second best results in the rural background areas are given by the variant (N), i.e. using EMEP model, altitude, wind speed and relative humidity as supplementary variables. Comparing the variants (L) and (L0), one can see that the logarithmic transformation gives a clear improvement, even if the land cover is included. (For the variant without the land cover inclusion, the similar conclusion was shown in Horálek et al. 2010.)

The findings concerning the improvement of the rural mapping if land cover data of natural areas are included confirm the conclusion of Horálek et al. (2010).

In the urban background areas, the best results are given for the variants (C) and (C1) using EMEP model output as supplementary data only, with slightly better performance for the current method (C) in 10x10 km². However, it should be noted that the original EMEP model output is already in about 10x10 km² grid resolution (see Section 3.2), meaning that the differences between (C) and (C1) should be minor only and caused mainly by the spatial re-aggregation from the EMEP model grid into either the somewhat different EEA 10x10 km² grid under (C) or the EEA 1x1 km² grid under (C1). Having a closer look at the results, we conclude that the differences between (C) and (C1) are highly influenced by several stations in the Balkan at highly polluted urban areas, where the different resulting grid resolutions derived from the original EMEP model grid resolution and projection under (C) and (C1) plays a role. One can conclude that the differences between (C) and (C1) are quite random and may be ignored.

Conclusion

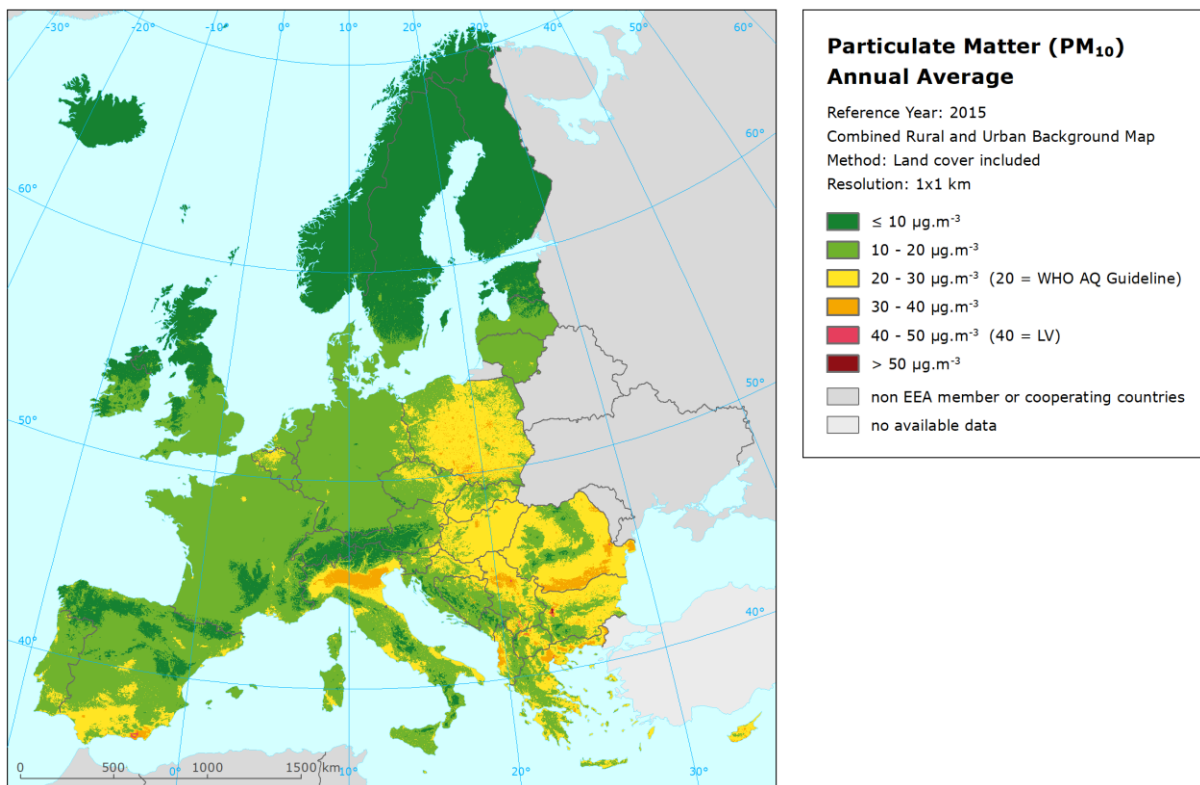
Based on the analysis results, it can be concluded that the inclusion of the land cover provides clear improvement on the PM₁₀ mapping methodology in the rural areas. Therefore, it is recommended to implement this supplementary data sources in the routine methodology to calculate the rural background map layer. When introducing this, it is recommended to also move the application of the 1x1 km² resolution to its earliest stage of the 'regression – kriging – merging' mapping process, i.e. moving it from the combined final merging process-step to the early process-step of the regression and kriging stage when creating each separate rural and urban background map layer. It is recommended to do this change of resolution for both rural and urban background map layers to assure methodological consistency at all

map layers. Thus, it is recommended to use (L) variant for the rural map layer and (C1) variant for the urban map layer in the updated methodology.

Mapping results

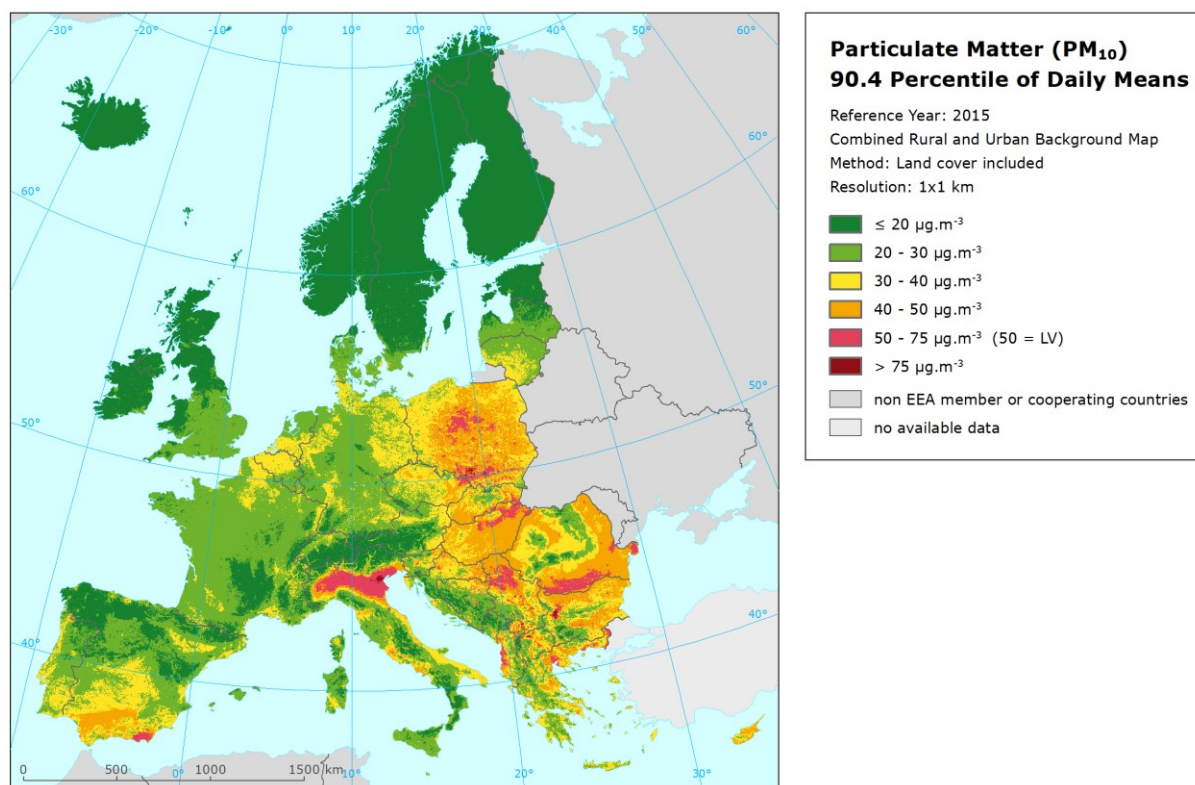
Map 4.1 presents the rural and urban background merged map of PM₁₀ annual average, created by the merge of rural and urban background map layers according to Equation 2.1. For the rural map layer, variant (L) is used. It should be noted that at limited areas with the lack of CLC2006 data (Andorra, Faroes, Jan Mayen), variant (L) cannot be used. At these cases we substitute the estimated rural map layer value with the value of the variant (N). For the urban background layer, variant (C1) is used.

Map 4.1 Concentration map of PM₁₀ annual average, rural and urban background merged map using method with land cover data, 2015. Rural map layer was created by (L) variant, while urban background map layer by (C1) variant.



Map 4.2 shows the rural and urban background merged map of PM₁₀ indicator 90.4 percentile of daily means, created similarly like Map 4.1.

Map 4.2 Concentration map of PM₁₀ indicator 90.4 percentile of daily means, rural and urban background merged map using method with land cover data, 2015. Rural map layer was created by (L) variant, urban background map layer by (C1) variant.



4.1.2 Traffic map layers

For the inclusion of the traffic map layer in the PM₁₀ mapping process, similar reasons as for NO₂ mapping play a role, see Horálek et al. (2017). So far, only background PM₁₀ maps (representing both rural and urban background areas) have been constructed, not including the monitoring information from traffic stations. However, traffic is an important source of PM₁₀ emissions. Therefore, we do estimate the traffic related air quality by using PM₁₀ measurement data from the traffic stations and available supplementary data, i.e. we create a traffic map layer. When the traffic map layer is ready, it can be included in the merging process to come to a final map (see Section 4.1.3). Due to the lack of data from rural traffic stations we concentrated on the urban traffic stations only.

In order to see the level of the “urban traffic increment”, we compared the measurement data at the urban traffic stations with the underlying urban background map layer. In average, the urban traffic/background ratio is 1.19 for annual average and 1.18 for 90.4 percentile of daily means. This is lower urban traffic/background ratio than in the case of NO₂, being 1.60 (calculated based on 2015 data used in Horálek et al., 2018). However, the level of this ratio justifies the separate construction of the urban traffic layer.

For the creation of the urban traffic map layer, we examined and mutually compared a similar set of mapping variants like for background areas. We have chosen as a baseline the variant (C1) using the same supplementary data as at the variant (C1) at the urban background mapping layer, i.e. EMEP model output. We apply the 1x1 km² resolution, we label this as (C1). Table 4.6 provides the overview of all the mutually compared variants.

Table 4.6 List of mutually compared variants of the mapping method, rural and urban background areas

Lab.	Variants Description	Area type	Grid resolution	EMEP	Alt.	Meteo	Popul. density	Land cover
(C1)	Like current UB, 1x1 km ²	Urban traffic	1x1 km ²	+	-	-	-	-
(L)	Land cover included	Urban traffic	1x1 km ²	+	+	+	-(^a)	-(^a)
(L0)	Land cover included, without lognormal transposition	Urban traffic	1x1 km ²	+	+	+	-(^a)	-(^a)
(N)	Without land cover	Urban traffic	1x1 km ²	+	+	+	-(^a)	-

(^a) Excluded in the backward stepwise selecting procedure

Table 4.7 presents for both PM₁₀ indicators the supplementary variables ultimately selected by the backward stepwise selection procedure and further applied, including their relevant statistical performance parameters at both the multiple linear regression and the subsequent interpolation by ordinary kriging of its residuals. It can be seen that quite surprisingly, no land cover data have been selected as significant performance contributors, leading to same results for both variants (N) and (L), which we further call ‘optimal’.

Table 4.7 Parameters of the linear regression models and of the ordinary kriging (nugget, sill, range) of PM₁₀ indicators annual average (left) and 90.4 percentile of daily means (right) for 2015 in urban traffic areas for different mapping variants

Linear Regr. Model + OK of its residuals	PM ₁₀ – annual average				PM ₁₀ – 90.4 percentile of daily means			
	(C1) Like current 1x1	(L) LC included	(L0) LC incl., no log. tr.	(N) Without LC	(C1) Like current 1x1	(L) LC included	(L0) LC incl., no log. tr.	(N) Without LC
	urb. tr. coeff.	urb. tr. coeff.	urb. tr. coeff.	urb. tr. coeff.	urb. tr. coeff.	u. tr. coeff.	u. tr. coeff.	urb. tr. coeff.
c (constant)	2.21	2.68	26.03	2.68	2.55	3.16	51.98	3.16
a1 (EMEP model)	0.368	0.327	0.526	0.327	0.354	0.301	0.401	0.301
a2 (altitude_1km)								
a3 (altit_5km_r)		-0.0003	-0.0071	-0.0003		-0.0003	-0.0158	-0.0003
a4 (wind speed)		-0.083	-2.131	-0.083		-0.103	-4.967	-0.103
a5 (NAT_1km)								
a6 (AGR_5km_r)								
Adjusted R²	0.37	0.44	0.37	0.44	0.31	0.40	0.33	0.40
St. Err. [µg.m⁻³]	0.237	0.223	6.06	0.223	0.271	0.254	12.66	0.254
Nugget	0.018	0.016	10	0.016	0.021	0.019	45	0.019
Sill	0.035	0.031	22	0.031	0.052	0.043	113	0.043
R	380	350	390	350	350	300	280	300

Note: Dark grey indicates variables not considered in the variant of the linear regression model. Light grey indicates variables not selected in the variant by the selecting procedure.

Comparison by cross-validation

Table 4.8 presents the mapping results of all variants for PM₁₀ annual average, with their different sets of supplementary data that are mutually compared by means of the ‘leave one out’ cross-validation (Section 2.3), for the urban traffic areas. Table 4.9 presents the similar table for PM₁₀ indicator 90.4 percentile.

Table 4.8 Comparison of different method variants of spatial interpolation showing RMSE, RRMSE, bias, R² and linear regression from the cross-validation scatter plots for PM₁₀ annual mean in urban traffic areas, 2015. Units: µg.m⁻³ except RRMSE and R².

Spatial interpolation variant + supplementary data used		Urban traffic areas				
		RMSE	RRMSE	Bias	R ²	Regr. eq.
(C1)	Like current, 1x1 km (EMEP)	5.1	20.7%	-0.2	0.612	y = 0.624x + 9.1
(L) = (N)	Optimal, 1x1 km (EMEP, altitude_5km_r, wind speed)	4.9	20.2%	-0.2	0.627	y = 0.646x + 8.5
(L0)	No log. trans., 1x1 km (EMEP, altitude_5km_r, wind sp.)	5.0	20.5%	-0.1	0.629	y = 0.664x + 8.1

Table 4.9 Comparison of different method variants of spatial interpolation showing RMSE, RRMSE, bias, R² and linear regression from the cross-validation scatter plots, PM₁₀ indicator 90.4 percentile of daily means in urban traffic areas, 2015. Units: µg.m⁻³ except RRMSE and R².

Spatial interpolation variant + supplementary data used		Urban traffic areas				
		RMSE	RRMSE	Bias	R ²	Regr. eq.
(C1)	Like current, 1x1 km (EMEP)	11.0	26.4%	-0.4	0.591	y = 0.602x + 16.5
(L) = (N)	Optimal, 1x1 km (EMEP, altitude_5km_r, wind speed)	10.7	25.6%	-0.4	0.613	y = 0.620x + 15.6
(L0)	No log. trans., 1x1 km (EMEP, altitude_5km_r, wind sp.)	10.9	26.0%	-0.2	0.611	y = 0.649x + 14.5

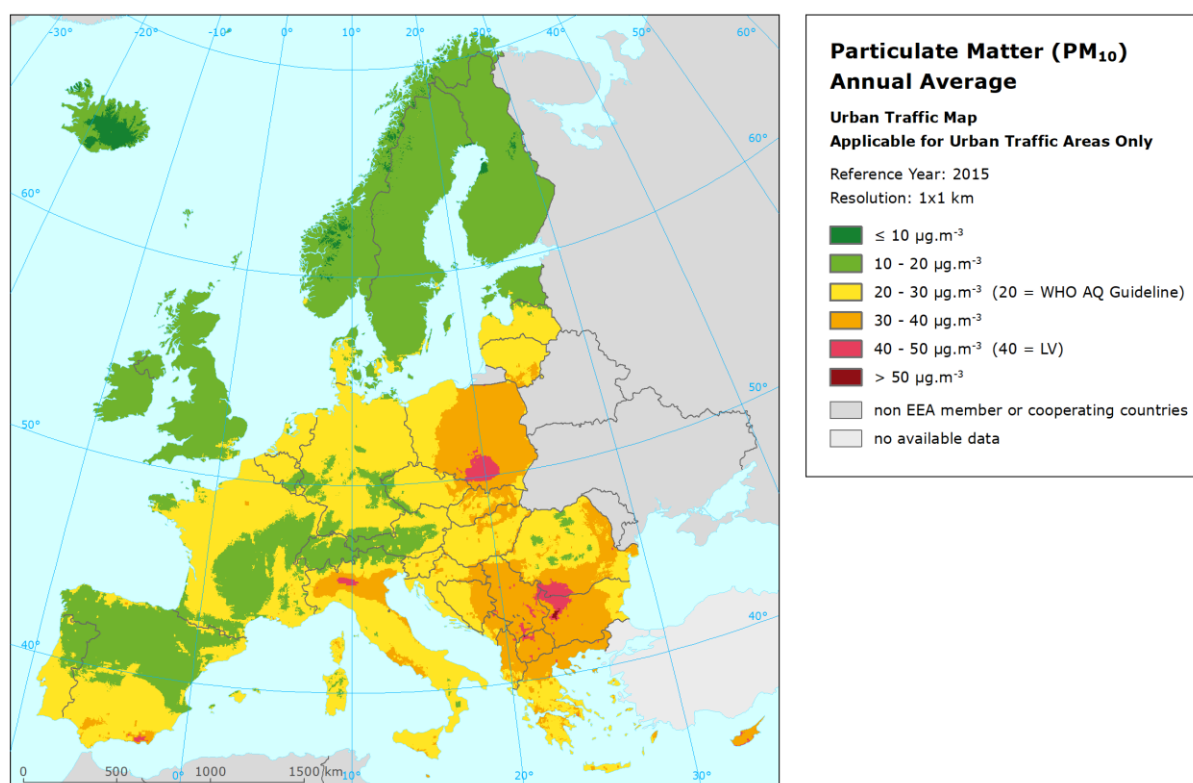
It can be seen that the best results in the urban traffic areas are given by the variants using EMEP model output, altitude and wind speed, for both PM₁₀ indicators, with slightly better RMSE results for the variant with the logarithmic transformation, i.e. (L) = (N). The relative RMSE of this method is about 20 % and 26 % respectively, meaning that the traffic map layers give quite reliable estimates for the urban traffic air quality and can be routinely applied.

Mapping results

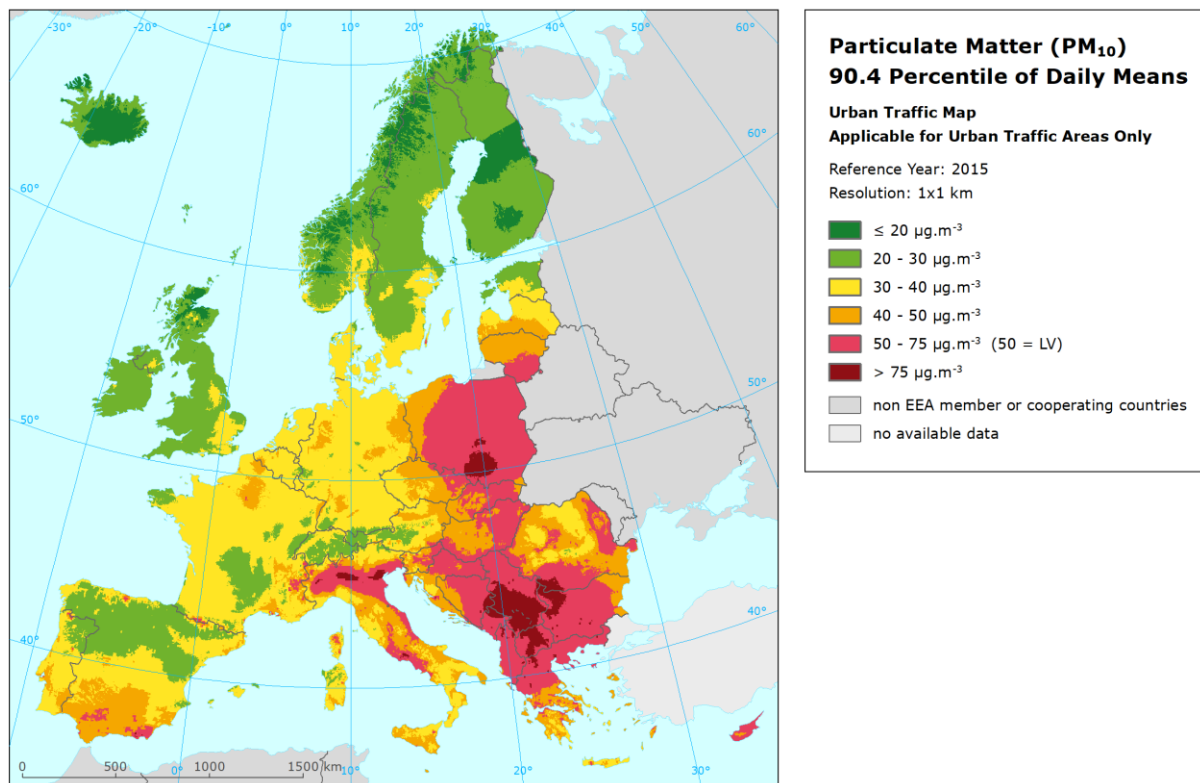
Based on the method (N), i.e. using measurement data from urban/suburban traffic stations as primarily data and EMEP model output, altitude and wind speed as supplementary data, urban traffic map layers have been prepared. It should be noted that at limited areas, the urban traffic map layer may provide lower concentration values than the urban background map layer, i.e. variant (C1) of Section 4.1. The reason is mostly the lack of either urban traffic or urban background stations in the given area. At these cases we substitute the estimated urban traffic map layer value with the higher value of this urban background map.

Maps 4.3 and 4.4 present the urban traffic map layers for PM₁₀ indicators annual average and 90.4 percentile of daily means for 2015, respectively. The maps are applicable for urban traffic areas only.

Map 4.3 Concentration map of PM₁₀ annual average, urban traffic air quality, 2015. Variant (L) = (N) was used. Applicable for urban traffic areas only.



Map 4.4 Concentration map of PM₁₀ indicator 90.4 percentile of daily means, urban traffic air quality, 2015. Variant (L) = (N) was used. Applicable for urban traffic areas only, 2015



4.1.3 Final concentration maps

The traffic map layers as prepared in Section 4.1.2 should be integrated with the rural and urban background map layers of Section 4.1.1. This should be done on basis of Equation 2.7, introduced in Section 2.3. As the traffic map layer represents the urban traffic areas, it is incorporated as part of the urban map layer together with the urban background map layer. Such urban layer is subsequently merged with the rural map layer into the combined final map. The crucial factor in this inclusion of the traffic map layer is the weight of the traffic map layer $w_T(i)$ (see Equation 2.7), which is based on the buffers around the roads.

In Horálek et al. (2017), the weight of the traffic map layer was established for NO₂ mapping. With a large degree of simplification, the size of the buffers around the roads representing the area influenced by urban traffic was set to 50 m for road class 3, resp. 75 m for road classes 1 and 2. The weight is calculated based on these buffers: the ratio of area influenced by traffic in a grid cell is divided by two. For motivation and further discussion, see Horálek et al. (2017). In the Annex, a brief literature review on the spatial gradients of NO₂ and PM concentrations along the roads is provided. Based on this literature review and a dispersion modelling exercise (see Annex, Section A.3), it seems to be an appropriate assumption that the horizontal spatial gradient as a function of distance from a major road is relatively similar for both NO₂ and PM₁₀. Leading from this, similar weighting for merging the urban traffic with the urban background map layer as applied in NO₂ mapping (see Horálek et al., 2017) has been applied for PM₁₀ mapping as well. Thus, the weight is applied according to

$$w_T(i) = T123buf_1km(i) / 2 \quad (4.1)$$

where $w_T(i)$ is the traffic weight of Equation 2.7 for grid cell i ,
 $T123buf_1km(i)$ is the ratio of area influenced by urban traffic in grid cell i , for road classes 1 – 3,

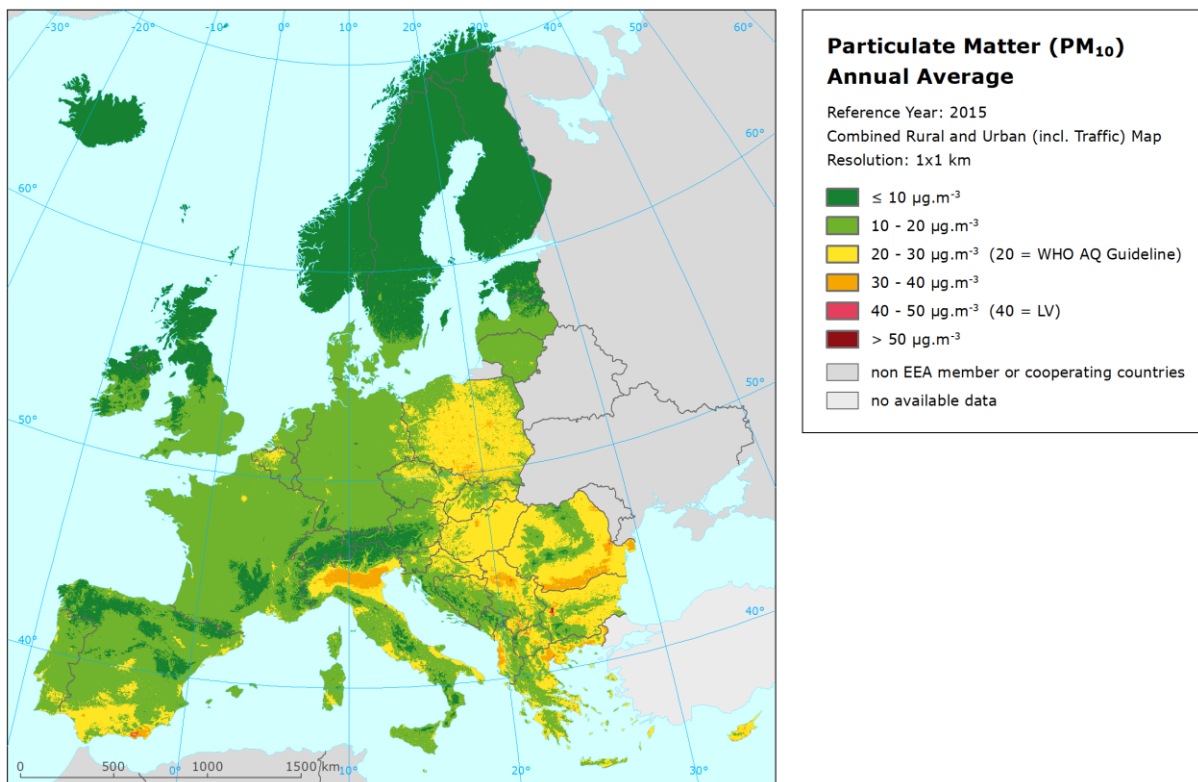
Mapping results

Map 4.5 presents the final concentration map of PM₁₀ annual average for 2015 created by including the traffic map layer as presented in Map 4.3 in the rural and urban background map of annual average as presented in Map 4.1.

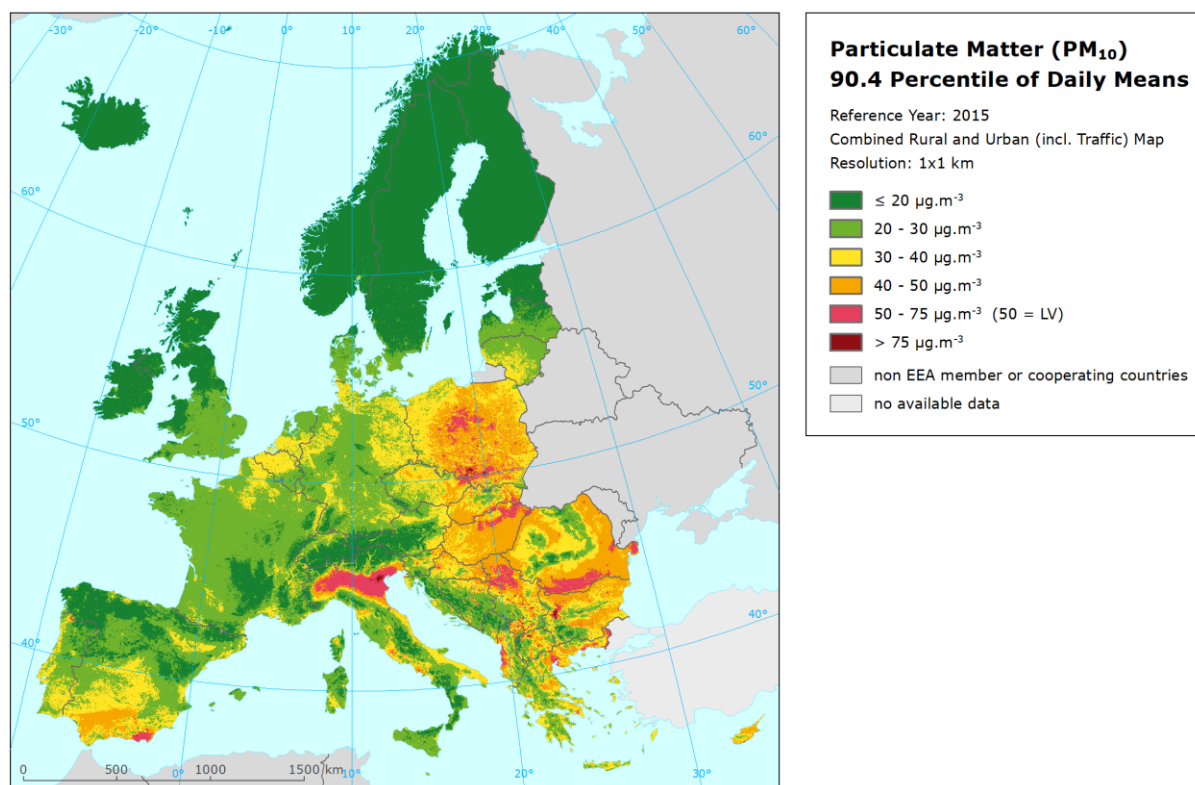
Map 4.6 presents the similar final concentration map of PM₁₀ indicator 90.4 percentile of daily means for 2015, i.e. created by including the traffic map layer as presented in Map 4.4 in the relevant rural and urban background map as presented in 4.2.

In terms of mapping variants, (L) variant is used for the rural map layer, (C1) variant for the urban background, and (L) = (N) variant for the urban traffic map layers, for both PM₁₀ indicators. It is recommended to apply these variants in the routine PM₁₀ mapping methodology.

Map 4.5 Concentration map of PM₁₀ annual average using method with land cover data and traffic map layer included, 2015



Map 4.6 Concentration map of PM₁₀ indicator 90.4 percentile of daily means using method with land cover data and traffic map layer included, 2015



Uncertainty estimates

Next to the cross-validation uncertainty estimates for the different mapping layers (see Tables 4.4 and 4.8 for annual average, resp. Tables 4.5. and 4.9 for 90.4 percentile of daily means, for the relevant map variants), a simple comparison between the point observation values and interpolated prediction values spatially averaged at 1x1 km² grid cells has been made. The comparison has been made both for the separate (i.e. rural, urban background resp. urban traffic) map layers, for the background merged map and for the final merged map. Table 4.10 presents the results of this comparison, together with the results of cross-validation prediction for the relevant map layers, for PM₁₀ annual average.

Table 4.10 Statistical indicators from the scatter plots for the cross-validation scatter plots from separate (rural, urban background or urban traffic) map layers and for the predicted grid values from separate (rural, urban background or urban traffic) map layers, background merged map and final merged map versus the measurement point values for rural (top), urban background (middle) and urban traffic (bottom) stations for PM₁₀ annual average 2015.

Map layer		rural background stations				
		RMSE	RRMSE	bias	R ²	lin. r. equation
(L)	cross-valid. prediction, separate rural background map layer	2.9	17.3%	0.0	0.771	y = 0.788x + 3.5
	grid prediction, 1x1 km ² , separate rural background map layer	2.2	13.4%	-0.1	0.864	y = 0.828x + 2.7
(r-ub merged)	grid prediction, 1x1 km ² , background merged map	2.3	14.0%	0.2	0.852	y = 0.842x + 2.8
(r-ub-ut merged)	grid prediction, 1x1 km ² final merged map	2.3	14.0%	0.2	0.851	y = 0.845x + 2.8
Map layer		urban/suburban background stations				
		RMSE	RRMSE	bias	R ²	lin r. equation
(C1)	cross-valid. prediction, separate urban background map layer	4.7	19.8%	0.0	0.670	y = 0.673x + 7.8
	grid prediction, 1x1 km ² separate urban background map layer	3.7	15.7%	-0.3	0.798	y = 0.731x + 6.2
(r-ub merged)	grid prediction, 1x1 km ² , background merged map	3.9	16.6%	-0.5	0.773	y = 0.724x + 6.0
(r-ub-ut merged)	grid prediction, 1x1 km ² final merged map	4.0	16.8%	-0.2	0.767	y = 0.714x + 6.6
Map layer		urban/suburban traffic stations				
		RMSE	RRMSE	bias	R ²	lin. r. equation
(L) = (N)	cross-valid. prediction, separate urban traffic map layer	4.9	20.2%	-0.2	0.627	y = 0.646x + 8.5
	grid prediction, 1x1 km ² separate urban traffic map layer	3.7	15.3%	0.0	0.791	y = 0.740x + 6.4
(r-ub merged)	grid prediction, 1x1 km ² , background merged map	6.3	25.6%	-3.9	0.618	y = 0.631x + 5.3
(r-ub-ut merged)	grid prediction, 1x1 km ² final merged map	5.9	24.0%	-3.5	0.646	y = 0.643x + 5.5

Table 4.11 presents the similar results for the PM₁₀ indicator 90.4 percentile of daily means.

Looking at the uncertainty grid prediction results for different map layers, similar results are given for both PM₁₀ indicators, i.e. for the annual average and the 90.4 percentile of daily means. One can see that both rural and urban background areas (represented by rural background resp. urban/suburban background stations) are well represented in both the background merged and the final merged maps. However, this is not true for the urban traffic areas, which are well represented by the separate urban traffic map layer only. It is clearly seen that not only in the background merged map (created without the use of the traffic map layer), but also in the final merged map, urban traffic areas are underestimated. The level of the underestimation is cc. 4 µg.m⁻³ for annual average and cc. 6 µg.m⁻³ for the 90.4 percentile of daily means. The underestimation is caused by the 1x1 km² resolution of the maps, which is too coarse to distinguish the traffic urban air quality. This fact is needed to be taken into account in the exposure estimates (Section 4.1.4), as well as in potential estimates of area of exceedance. Thus, urban traffic areas should be dealt with separately in such types of analysis (like we do in Eq. 2.8 for population exposure).

Table 4.11 Statistical indicators from the scatter plots for the cross-validation scatter plots from separate (rural, urban background or urban traffic) map layers and for the predicted grid values from separate (rural, urban background or urban traffic) map layers, background merged map and final merged map versus the measurement point values for rural (top), urban background (middle) and urban traffic (bottom) stations for PM₁₀ annual average 2015.

Map layer		rural background stations				
		RMSE	RRMSE	bias	R ²	lin. r. equation
(L)	cross-valid. prediction, separate rural background map layer	5.6	19.1%	0.0	0.754	y = 0.781x + 6.4
	grid prediction, 1x1 km ² , separate rural background map layer	4.1	13.9%	-0.3	0.871	y = 0.830x + 4.7
(r-ub merged)	grid prediction, 1x1 km ² , background merged map	4.2	14.3%	0.3	0.863	y = 0.850x + 4.7
(r-ub-ut merged)	grid prediction, 1x1 km ² final merged map	4.2	14.3%	0.4	0.862	y = 0.851x + 4.7
Map layer		urban/suburban background stations				
		RMSE	RRMSE	bias	R ²	lin r. equation
(C1)	cross-valid. prediction, separate urban background map layer	10.8	25.7%	-0.1	0.632	y = 0.635x + 15.3
	grid prediction, 1x1 km ² separate urban background map layer	8.0	19.1%	-0.6	0.808	y = 0.719x + 11.2
(r-ub merged)	grid prediction, 1x1 km ² , background merged map	8.5	20.2%	-1.1	0.785	y = 0.701x + 11.5
(r-ub-ut merged)	grid prediction, 1x1 km ² final merged map	8.5	20.3%	-0.7	0.781	y = 0.692x + 12.3
Map layer		urban/suburban traffic stations				
		RMSE	RRMSE	bias	R ²	lin. r. equation
(L) = (N)	cross-valid. prediction, separate urban traffic map layer	10.7	25.6%	-0.4	0.613	y = 0.620x + 15.6
	grid prediction, 1x1 km ² separate urban traffic map layer	7.8	18.8%	0.0	0.805	y = 0.738x + 11.1
(r-ub merged)	grid prediction, 1x1 km ² , background merged map	12.7	30.4%	-6.7	0.607	y = 0.615x + 10.1
(r-ub-ut merged)	grid prediction, 1x1 km ² final merged map	12.1	28.9%	-6.0	0.635	y = 0.626x + 10.3

4.1.4 Exposure estimates

Next to the concentration maps, population exposure estimates have been created for both PM₁₀ indicators. The final population exposure is calculated using Equation 2.8, which distinguishes between the background and urban traffic areas, i.e. in agreement with the discussion of Tables 4.10 and 4.11. The weight $w_T(i)$ is calculated according to Equation 4.1. The separate use of the urban traffic map layer in the Equation 2.8 guarantees the concentrations used for the population exposure are not smoothed inside the 1x1 km² grid cells, which would lead into the underestimation of the population exposure.

Table 4.12 presents the final population exposure estimate of PM₁₀ annual average for 2015, based on the method with land cover data and traffic map layer included. In this estimate, the rural and urban background annual average map as presented in Map 4.1 and the urban traffic map layer as presented in Map 4.3 are used. Table 4.13 presents the similar final population exposure estimate of PM₁₀ indicator 90.4 percentile of daily means for 2015. In this estimate, the relevant rural and urban background map as presented in Map 4.2 and the urban traffic map layer as presented in Map 4.4 are used.

Table 4.14 shows the comparison of the final exposure estimate for PM₁₀ annual average for 2015 as presented in Table 4.12 (labelled "Final T.4.12") with the exposure estimate calculated based on the rural and urban background merged map as presented in Map 4.1 (labelled "Background M. 4.1"), as well as with the current approach (Section 2.1) as presented in Horálek et al. (2018) (labelled "Current TP17/7"). In the current method, (C) variants of both rural and urban background map layers are applied. For all three methods, the percentage of population living above LV is presented, as well as the population-weighted concentration. The method presented in Table 4.12 (i.e. with the most realistic results) is marked by dark orange. The method presented in Map 4.1 is marked by light orange.

Next to the results for the individual methods, the difference between "Background" and "Current" results, as well as between "Final" and "Background" results are presented. Comparing the "Background" and "Current" results one can see the effect of inclusion the land cover data in the mapping. The

comparison of “Final” and “Background” results show the effect of inclusion of the urban traffic map layer in the mapping.

Table 4.12 Population exposure and population-weighted concentration using method with land cover data and traffic map layer included, PM₁₀ annual average, 2015

Country	Population [inhbs . 1000]	PM ₁₀ annual average, exposed population [%]						Population weighted conc. [µg.m ⁻³]	
		< LV				> LV			
		< 10 µg.m ⁻³	10 - 20 µg.m ⁻³	20 - 30 µg.m ⁻³	30 - 40 µg.m ⁻³	40 - 45 µg.m ⁻³	> 45 µg.m ⁻³		
Albania	AL	2 892	0.0	4.3	22.2	72.8	0.7	31.7	
Andorra	AD	78	0.2	13.6	86.2			24.0	
Austria	AT	8 576	2.0	54.0	44.1			19.0	
Belgium	BE	11 237		34.6	65.4			20.5	
Bosnia & Herzegovina	BA	3 825	0.1	16.4	46.1	37.4	0.0	26.6	
Bulgaria	BG	7 202	0.0	1.7	25.6	57.0	14.9	33.9	
Croatia	HR	4 225	0.0	9.9	80.9	9.2		25.3	
Cyprus	CY	1 173		0.2	13.6	83.1	3.0	33.0	
Czechia	CZ	10 538	0.0	16.4	74.7	8.9	0.0	23.5	
Denmark	DK	5 660	0.4	97.7	1.9			17.2	
Estonia	EE	1 315	17.5	82.4	0.1			12.5	
Finland	FI	5 472	59.1	40.9				9.4	
France (metropolitan)	FR	64 344	0.4	73.1	25.3	1.3		18.8	
Germany	DE	81 198	0.1	86.9	13.0			18.3	
Greece	GR	10 858		2.3	46.7	43.7	7.4	30.7	
Hungary	HU	9 856		0.2	79.9	19.9		27.4	
Iceland	IS	329	42.2	57.5	0.3			10.2	
Ireland	IE	4 629	13.3	86.7				12.3	
Italy	IT	60 796	0.2	9.0	64.8	25.6	0.4	26.7	
Latvia	LV	1 986	1.0	75.1	22.8	1.1		17.3	
Liechtenstein	LI	37	0.9	99.1				16.5	
Lithuania	LT	2 921		61.5	35.7	2.7		19.4	
Luxembourg	LU	563		87.6	12.4			18.7	
Malta	MT	429		1.2	88.6	10		26.5	
Monaco	MC	38			100.0			23.8	
Montenegro	ME	622	0.5	14.1	58.5	23.9	3.0	27.1	
Netherlands	NL	16 901		81.7	18.3			18.9	
North Macedonia	MK	2 069	0.0	0.7	4.1	70.9	24.1	37.5	
Norway	NO	5 166	40.5	57.8	1.7			11.3	
Poland	PL	38 006	0.0	3.0	44.5	51.0	1.5	29.9	
Portugal (excl. Az., Mad.)	PT	9 870	0.2	59.2	39.8	0.8		19.3	
Romania	RO	19 871	0.0	4.9	67.6	27.2	0.3	26.5	
San Marino	SM	33		5.3	94.7			24.7	
Serbia (incl. Kosovo*)	RS	8 919	0.0	2.2	23.0	68.5	6.2	33.3	
Slovakia	SK	5 421	0.0	1.8	82.5	15.6		26.7	
Slovenia	SI	2 063	0.0	19.3	78.7	2.0		23.6	
Spain (excl. Canarias)	ES	44 323	0.6	34.5	59.0	5.8	0.1	22.1	
Sweden	SE	9 747	22.4	76.2	1.4			13.5	
Switzerland	CH	8 238	2.4	86.3	11.3	0.0		17.6	
United Kingdom (& dep.)	UK	64 875	1.9	96.6	1.5			15.2	
Total	536 303	2.0	50.0	34.2	13.0	0.7	0.0	21.6	
		52.0				0.7			
EU-28	504 055	1.7	51.0	35.2	11.6	0.6	0.0	21.4	
		52.7				0.6			
Kosovo*	KS	1 805	0.0	2.0	16.8	56.0	25.2	0.0	34.8
Serbia (excl. Kosovo*)	RS	7 114	0.0	2.2	24.6	71.6	1.6		32.2

*) under the UN Security Council Resolution 1244/99

Note 1: Turkey is not included in the calculation due to the lack of air quality data.

Note 2: The percentage value "0.0" indicates that an exposed population exists, but it is small and estimated lesser than 0.05 %.

Empty cells mean: no population in exposure.

Table 4.13 Population exposure and population-weighted concentration using method with land cover data and traffic map layer included, PM₁₀ indicator 90.4 percentile of daily means, 2015

Country	Population [inhbs . 1000]	PM ₁₀ , 90.4 percentile of daily means, exposed population [%]						Pop. weighted conc. [µg.m ⁻³]	
		< LV				> LV			
		< 20 µg.m ⁻³	20 - 30 µg.m ⁻³	30 - 40 µg.m ⁻³	40 - 50 µg.m ⁻³	50 - 75 µg.m ⁻³	> 75 µg.m ⁻³		
Albania	AL	2 892	0.0	1.9	7.5	13.1	75.8	1.6	57.7
Andorra	AD	78	0.2	9.4	12.4	78.0	0.0	0.0	44.2
Austria	AT	8 576	2.9	23.2	64.9	9.0	0.0	0.0	33.1
Belgium	BE	11 237	0.0	5.1	93.3	1.5	0.0	0.0	34.8
Bosnia & Herzegovina	BA	3 825	0.3	7.8	13.9	14.3	62.1	1.6	53.0
Bulgaria	BG	7 202	0.0	0.6	3.8	21.7	56.3	17.5	63.2
Croatia	HR	4 225	0.1	4.1	14.6	40.0	41.3	0.0	46.9
Cyprus	CY	1 173	0.0	0.1	3.7	83.2	13.0	0.0	48.1
Czechia	CZ	10 538	0.0	2.8	46.5	38.1	12.5	0.0	41.9
Denmark	DK	5 660	1.5	43.6	54.9	0.0	0.0	0.0	29.5
Estonia	EE	1 315	29.3	69.9	0.8	0.0	0.0	0.0	21.3
Finland	FI	5 472	95.3	3.7	1.0	0.0	0.0	0.0	15.6
France (metropolitan)	FR	64 344	1.2	42.3	53.0	2.8	0.7	0.0	31.0
Germany	DE	81 198	0.2	34.7	63.2	1.9	0.1	0.0	31.3
Greece	GR	10 858	0.0	1.4	24.0	34.0	33.8	6.9	50.3
Hungary	HU	9 856	0.0	0.0	2.5	61.1	36.4	0.0	48.4
Iceland	IS	329	93.5	4.7	1.8	0.0	0.0	0.0	15.4
Ireland	IE	4 629	31.9	68.0	0.1	0.0	0.0	0.0	21.9
Italy	IT	60 796	0.5	5.5	29.5	30.1	32.4	2.1	47.6
Latvia	LV	1 986	2.6	45.2	48.2	2.9	1.1	0.0	30.7
Liechtenstein	LI	37	1.2	27.0	71.8	0.0	0.0	0.0	29.5
Lithuania	LT	2 921	0.0	12.6	77.1	6.3	4.0	0.0	35.8
Luxembourg	LU	563	0.0	21.3	78.7	0.1	0.0	0.0	31.5
Malta	MT	429	0.0	1.0	3.1	96	0.0	0.0	41.4
Monaco	MC	38	0.0	0.0	100.0	0	0.0	0.0	35.6
Montenegro	ME	622	1.1	10.0	7.7	8.9	64.1	8.2	53.5
Netherlands	NL	16 901	0.0	39.8	60.2	0	0.0	0.0	30.7
North Macedonia	MK	2 069	0.0	0.4	1.1	2.5	29.5	66.6	77.5
Norway	NO	5 166	45.5	45.2	8.6	0.7	0.0	0.0	19.7
Poland	PL	38 006	0.0	0.1	7.1	28.0	56.2	8.7	56.1
Portugal (excl. Az., Mad.)	PT	9 870	0.8	23.0	70.7	5.5	0.2	0.0	33.0
Romania	RO	19 871	0.0	0.8	26.2	47.4	25.4	0.1	44.8
San Marino	SM	33	0.0	0.4	11.7	87	1.3	0.0	44.4
Serbia (incl. Kosovo*)	RS	8 919	0.0	1.1	3.8	11.4	51.1	32.7	65.8
Slovakia	SK	5 421	0.0	0.2	6.9	57.2	35.6	0.0	47.9
Slovenia	SI	2 063	0.0	7.3	26.3	44.4	22.0	0.0	43.0
Spain (excl. Canarias)	ES	44 323	1.3	20.4	57.7	18.3	2.2	0.0	35.6
Sweden	SE	9 747	28.6	60.4	10.8	0.3	0.0	0.0	22.8
Switzerland	CH	8 238	3.1	34.9	59.4	2.2	0.4	0.0	30.6
United Kingdom (& dep.)	UK	64 875	3.9	92.8	3.2	0.0	0.0	0.0	25.6
Total	536 303	3.2	29.7	36.6	14.3	14.1	2.1	37.5	
				83.8		16.2			
EU-28	504 055	2.9	30.5	37.6	14.8	13.0	1.3	36.9	
				85.7		14.3			
Kosovo*	KS	1 805	0.0	0.7	5.6	7.5	25.6	60.6	72.4
Serbia (excl. Kosovo*)	RS	7 114	0.0	1.2	3.4	12.3	57.3	25.9	64.2

Note 1: Turkey is not included in the calculation due to the lack of air quality data.

Note 2: The percentage value "0.0" indicates an exposed population exists, but it is small and estimated less than 0.05 %. Empty cells mean: no population in exposure.

Table 4.14 Population exposure above LV (left) and population-weighted concentration (right) using current method, method with land cover data included (Map 4.1) and method with LC data and traffic map layer included (Table 4.12), and differences between two methods, PM₁₀ annual average, 2015.

Country	Exposed population > LV [%]					Population-weighted concentration [$\mu\text{g}\cdot\text{m}^{-3}$]					
	Current TP'17/7	Backgr. M. 4.1	Differ. Back. -C.	Final T. 4.12	Differ. Fin.-Back.	Current TP'17/7	Backgr. M. 4.1	Differ. Back. -C.	Final T. 4.12	Differ. Fin.-Back.	
Albania	AL	0.6	0.7	0.0	0.7	0.0	30.2	31.7	1.4	31.7	0.0
Andorra	AD	0	0	0	0	0	24.7	24.0	-0.7	24.0	0.0
Austria	AT	0	0	0	0	0	18.7	18.7	0.1	19.0	0.3
Belgium	BE	0	0	0	0	0	20.4	20.3	0.0	20.5	0.2
Bosnia & Herzegovina	BA	0.0	0	0.0	0.0	0.0	26.8	26.6	-0.2	26.6	0.0
Bulgaria	BG	15.1	15.4	0.3	15.8	0.3	33.1	33.8	0.7	33.9	0.1
Croatia	HR	0	0	0	0	0	25.1	25.2	0.1	25.3	0.1
Cyprus	CY	0	0	0	3.0	3.0	31.4	32.5	1.1	33.0	0.5
Czechia	CZ	0	0	0	0.0	0.0	23.3	23.4	0.1	23.5	0.1
Denmark	DK	0	0	0	0	0	17.1	17.1	0.1	17.2	0.1
Estonia	EE	0	0	0	0	0	12.1	12.2	0.1	12.5	0.2
Finland	FI	0	0	0	0	0	9.1	9.1	0.0	9.4	0.2
France (metropolitan)	FR	0	0	0	0	0	18.2	18.4	0.2	18.8	0.4
Germany	DE	0	0	0	0	0	17.8	18.0	0.2	18.3	0.3
Greece	GR	5.4	5.9	0.5	7.4	1.5	28.7	30.5	1.7	30.7	0.3
Hungary	HU	0	0	0	0	0	26.3	27.3	1.0	27.4	0.1
Iceland	IS	0	0	0	0	0	9.7	9.8	0.1	10.2	0.4
Ireland	IE	0	0	0	0	0	11.9	12.1	0.2	12.3	0.1
Italy	IT	0	0	0	0.4	0.4	26.6	26.5	-0.1	26.7	0.2
Latvia	LV	0	0	0	0	0	16.5	17.0	0.5	17.3	0.4
Liechtenstein	LI	0	0	0	0	0	16.3	16.5	0.2	16.5	0.0
Lithuania	LT	0	0	0	0	0	18.5	18.8	0.3	19.4	0.6
Luxembourg	LU	0	0	0	0	0	18.5	18.5	0.0	18.7	0.3
Malta	MT	0	0	0	0	0	26.4	25.9	-0.5	26.5	0.6
Monaco	MC	0	0	0	0	0	23.2	23.1	-0.1	23.8	0.7
Montenegro	ME	3.0	3.0	0.0	3.0	0.0	26.7	27.0	0.4	27.1	0.1
Netherlands	NL	0	0	0	0	0	18.7	18.7	0.1	18.9	0.2
North Macedonia	MK	29.9	24.3	-5.6	24.4	0.0	37.3	37.5	0.2	37.5	0.0
Norway	NO	0	0	0	0	0	11.1	11.0	-0.1	11.3	0.3
Poland	PL	1.3	1.0	-0.3	1.5	0.5	29.5	29.8	0.3	29.9	0.1
Portugal (excl. Az., Mad.)	PT	0	0	0	0	0	18.7	19.1	0.4	19.3	0.2
Romania	RO	0	0.0	0.0	0.3	0.2	25.7	26.3	0.6	26.5	0.2
San Marino	SM	0	0	0	0	0	24.6	24.6	0.0	24.7	0.1
Serbia (incl. Kosovo*)	RS	3.0	5.9	2.9	6.2	0.3	32.7	33.2	0.5	33.3	0.0
Slovakia	SK	0	0	0	0	0	26.3	26.5	0.2	26.7	0.1
Slovenia	SI	0	0	0	0	0	23.3	23.4	0.1	23.6	0.1
Spain (excl. Canarias)	ES	0.1	0.1	0.0	0.1	0.0	21.6	22.0	0.3	22.1	0.1
Sweden	SE	0	0	0	0	0	13.3	13.3	0.0	13.5	0.2
Switzerland	CH	0	0	0	0	0	17.4	17.5	0.1	17.6	0.1
United Kingdom (& dep.)	UK	0	0	0	0	0	15.1	15.1	0.0	15.2	0.2
Total		0.6	0.6	0.0	0.7	0.1	21.2	21.4	0.2	21.6	0.2
EU-28		0.4	0.4	0.0	0.6	0.1	20.9	21.2	0.2	21.4	0.2
Kosovo*	KS	12.7	25.2	12.5	25.2	0.0	34.8	35.6	0.8	35.6	0.0
Serbia (excl. Kosovo*)	RS	0.6	1.2	0.6	1.6	0.4	32.2	32.6	0.5	32.7	0.1

*) under the UN Security Council Resolution 1244/99

Note 1: Turkey is not included in the calculation due to the lack of air quality data.

Note 2: The percentage value "0.0" indicates that an exposed population exists, but it is small and estimated lesser than 0.05 %. The percentage value "0" mean: no population in exposure.

Table 4.15 Population exposure above LV (left) and population-weighted concentration (right) using current method, method with land cover data included (Map 4.1) and method with LC data and traffic map layer included (Table 4.13), and differences between two methods, PM₁₀ indicator 90.4 percentile of daily means, 2015.

Country	Exposed population > LV [%]					Population-weighted concentration [$\mu\text{g}\cdot\text{m}^{-3}$]					
	Current TP'17/7	Backgr. M. 4.3	Differ. Back. -C.	Final T. 4.13	Differ. Fin.-Back.	Current TP'17/7	Backgr. M. 4.3	Differ. Back. -C.	Final T. 4.13	Differ. Fin.-Back.	
Albania	AL	73.5	77.3	3.8	77.4	0.1	56.6	57.6	1.0	57.7	0.1
Andorra	AD	9.7	0	-9.7	0	0.0	45.7	44.2	-1.5	44.2	0.0
Austria	AT	0	0	0	0.0	0.0	32.4	32.6	0.2	33.1	0.5
Belgium	BE	0	0	0	0	0	34.6	34.7	0.0	34.8	0.1
Bosnia & Herzegovina	BA	64.3	63.6	-0.8	63.7	0.1	54.5	53.0	-1.4	53.0	0.0
Bulgaria	BG	71.4	73.8	2.4	73.8	0.1	62.2	63.2	1.0	63.2	0.1
Croatia	HR	42.5	40.3	-2.3	41.3	1.0	46.8	46.6	-0.2	46.9	0.3
Cyprus	CY	0	5.0	5.0	13.0	7.9	45.2	47.0	1.7	48.1	1.1
Czechia	CZ	12.1	12.1	0.0	12.5	0.4	41.6	41.7	0.2	41.9	0.1
Denmark	DK	0	0	0	0	0	29.3	29.4	0.1	29.5	0.1
Estonia	EE	0	0	0	0	0	20.7	20.9	0.3	21.3	0.4
Finland	FI	0	0	0	0	0	15.0	15.1	0.1	15.6	0.4
France (metropolitan)	FR	0.0	0.0	0.0	0.7	0.6	30.2	30.5	0.2	31.0	0.5
Germany	DE	0.1	0.1	0.0	0.1	0.0	30.6	30.9	0.3	31.3	0.4
Greece	GR	29.5	37.7	8.2	40.6	2.9	48.2	49.7	1.5	50.3	0.6
Hungary	HU	19.3	35.1	15.8	36.4	1.4	46.2	48.2	2.0	48.4	0.1
Iceland	IS	0	0	0	0	0	14.5	14.5	0.0	15.4	0.9
Ireland	IE	0	0	0	0	0	21.3	21.7	0.3	21.9	0.2
Italy	IT	32.6	33.2	0.6	34.5	1.3	47.4	47.3	-0.1	47.6	0.3
Latvia	LV	0	0	0	1.1	1.1	29.0	30.0	1.1	30.7	0.6
Liechtenstein	LI	0	0	0	0	0	28.9	29.4	0.5	29.5	0.0
Lithuania	LT	0	0	0	4.0	4.0	34.0	34.8	0.9	35.8	1.0
Luxembourg	LU	0	0	0	0	0	31.1	31.1	0.0	31.5	0.3
Malta	MT	0	0	0	0	0	41.7	40.7	-1.0	41.4	0.6
Monaco	MC	0	0	0	0	0	35.0	35.0	0.0	35.6	0.5
Montenegro	ME	67.4	72.1	4.7	72.3	0.2	52.9	53.1	0.2	53.5	0.4
Netherlands	NL	0	0	0	0	0	30.2	30.4	0.2	30.7	0.3
North Macedonia	MK	94.9	96.0	1.1	96.0	0.0	78.1	77.5	-0.6	77.5	0.0
Norway	NO	0	0	0	0	0	19.3	19.1	-0.2	19.7	0.6
Poland	PL	63.1	64.4	1.3	64.8	0.4	55.7	56.0	0.3	56.1	0.1
Portugal (excl. Az., Mad.)	PT	0.0	0.0	0.0	0.2	0.2	31.8	32.7	0.9	33.0	0.3
Romania	RO	19.2	23.9	4.7	25.5	1.6	43.8	44.5	0.6	44.8	0.3
San Marino	SM	0	0	0	1.3	1.3	43.7	44.2	0.5	44.4	0.1
Serbia (incl. Kosovo*)	RS	80.2	83.6	3.4	83.8	0.2	65.7	65.8	0.1	65.8	0.0
Slovakia	SK	32.8	34.7	1.9	35.6	1.0	47.4	47.8	0.4	47.9	0.2
Slovenia	SI	22.5	20.4	-2.1	22.0	1.6	42.6	42.6	0.0	43.0	0.3
Spain (excl. Canarias)	ES	1.9	1.8	-0.2	2.2	0.4	34.9	35.4	0.5	35.6	0.2
Sweden	SE	0	0	0	0	0	22.4	22.4	0.1	22.8	0.3
Switzerland	CH	0.5	0.3	-0.2	0.4	0.2	30.1	30.5	0.4	30.6	0.2
United Kingdom (& dep.)	UK	0	0	0	0	0	25.3	25.3	0.0	25.6	0.3
Total		14.7	15.6	0.9	16.2	0.5	36.9	37.2	0.3	37.5	0.3
EU-28		12.9	13.7	0.9	14.3	0.5	36.2	36.5	0.3	36.9	0.3
Kosovo*	KS	83.4	86.2	2.7	86.2	0.0	71.2	72.4	1.1	72.4	0.0
Serbia (excl. Kosovo*)	RS	79.4	82.9	3.5	83.2	0.2	64.3	64.1	-0.2	64.2	0.0

*) under the UN Security Council Resolution 1244/99

Note 1: Turkey is not included in the calculation due to the lack of air quality data.

Note 2: The percentage value "0.0" indicates that an exposed population exists, but it is small and estimated lesser than 0.05 %. The percentage value "0" mean: no population in exposure.

Looking at the results, one can state that the differences between "Background" and "Current" results are small, except in the highly polluted areas (Balkan). This difference might be related to the higher resolution in the "Background" map, while in the "Current" map peaks might be smoothed in the 10x10 km grid. The differences in these areas are also influenced by small density of measuring stations.

Comparing the “Final” and “Background” results, one can see the effect of the traffic map layer inclusion. In the “Final” map the now included traffic contributions results in a further increase in concentrations.

As can be seen, the implementation of both land cover traffic map layer inclusions leads into quite limited increase in the estimate of the population-weighted concentration across Europe, which is cc. $0.4 \mu\text{g}\cdot\text{m}^{-3}$ for the annual average and cc. $0.6 \mu\text{g}\cdot\text{m}^{-3}$ for the 90.4 percentile of daily means. For the population exposure related to the concentration classes above LV, there is almost no increase for the annual average and cc. 1.4 % increase for the 90.4 percentile of daily means, if the updated methodology is applied.

As can be seen in Table 4.12 and in Horálek et al. (2018), according to the “Final” resp. “Current” results, 47 % resp. 45 % of the EU-28 population has been exposed to annual average concentrations above the Air Quality Guideline of $20 \mu\text{g}\cdot\text{m}^{-3}$ recommended by the World Health Organization (WHO, 2005). CSI004 (EEA, 2017b) estimates that about 52 % of the population in urban agglomerations in the EU-28 was exposed in 2015 to levels above the WHO guideline. The CSI004 estimate accounts for the *urban* population of the EU-28 (for which valid PM_{10} monitoring data has been reported), i.e. it represents areas where, in general, considerably higher PM_{10} concentrations occur compared to other areas. The estimates in Table 4.12 and in Horálek et al. (2018) account for the total EU-28 population, *including* the population in rural areas, smaller cities and villages that are in general exposed to lower levels of PM_{10} .

4.2 $\text{PM}_{2.5}$

4.2.1 Rural and urban background merged concentration map

Like in the case of PM_{10} , for both rural and urban background map layers, we have examined the inclusion of the land cover and road type data in the mapping process. We have compared the mapping variants without and with the inclusion of land cover and road type data.

As the basic variant, we have used the current methodology (Horálek et al., 2018a), labelled as (C), which is performed for the separate rural and urban background layers at a $10 \times 10 \text{ km}^2$ grid resolution (while a $1 \times 1 \text{ km}^2$ resolution is applied in the final merge of these map layers). For better comparability with the improved variant (see below) that is executed on $1 \times 1 \text{ km}^2$ in all mapping process steps, we again introduce also the so called ‘like current’ variant, labelled as (C1). In this (C1) variant, exactly the same set of supplementary variables as at variant (C) is applied (i.e. EMEP model output, altitude and wind speed in rural areas, and EMEP model output in the urban background areas), but contrary to (C) variant, (C1) is executed on a $1 \times 1 \text{ km}^2$ grid resolution in all mapping process steps.

The basic variants (C and C1) have been compared with a variant including the land cover data, labelled as (L). Additionally, we have examined also this variant including the land cover and road type data, but using the true $\text{PM}_{2.5}$ measurement data only, i.e. without the use of the data from the pseudo $\text{PM}_{2.5}$ stations that are normally applied in the $\text{PM}_{2.5}$ mapping (see Denby et al., 2011, Horálek et al., 2018); we label this variant as (LT). The reason for examination of this (LT) variant is to verify whether the inclusion of the pseudo $\text{PM}_{2.5}$ data improves the $\text{PM}_{2.5}$ mapping results even if additional supplementary data are included. The variant (L0), i.e. no log transformation, has not been tested, in view of the bad results obtained for PM_{10} .

Next to this, like in the case of PM_{10} , we have examined a variant ‘without the inclusion of land cover data’ labeled as (N), i.e. the variant using the most suitable supplementary data without inclusion of land cover data. In this variant, the selection procedure as described in Section 2.2 was applied for the whole set of supplementary variables apart from land cover parameters. For motivation, see Section 4.1.1.

The most useful supplementary data in (N), (L) and (LT) variants have been selected through a stepwise regression and backwards elimination (Section 2.2). Table 4.16 provides the overview of all the mutually compared variants, including their specific set of used supplementary data in terms of several classes of variables, as described in the introductory section of Chapter 4.

Table 4.16 List of mutually compared variants of the PM_{2.5} mapping method, rural and urban background areas

Lab.	Variant Description	Area type	Grid resolution	EMEP	Alt.	Meteo	Popul. density	Land cover
(C)	Current, 10x10 km ²	Rural background	10x10 km ²	+	+	+	-	-
		Urban background	10x10 km ²	+	-	+	-	-
(C1)	Like current, 1x1 km ²	Rural background	1x1 km ²	+	+	+	-	-
		Urban background	1x1 km ²	+	-	+	-	-
(L)	Land cover included	Rural background	1x1 km ²	+	+	+	-(^a)	+
		Urban background	1x1 km ²	+	-(^a)	+	-(^a)	+
(LT)	Land cover included, without pseudo PM _{2.5} stations	Rural background	1x1 km ²	+	+	+	-(^a)	+
		Urban background	1x1 km ²	+	-(^a)	+	-(^a)	+
(N)	Without land cover	Rural background	1x1 km ²	+	+	+	-(^a)	-
		Urban background	1x1 km ²	+	-(^a)	+	-(^a)	-

(^a) Excluded in the backward stepwise selecting procedure

Table 4.17 presents the supplementary variables ultimately selected and applied, including their relevant statistical performance parameters at both the multiple linear regression and the subsequent interpolation by ordinary kriging of its residuals, for the PM_{2.5} annual average.

For the variant including land cover (L), the selected variables are EMEP model output, altitude, wind speed, and the land cover parameter NAT_1km in the rural areas, resp. EMEP model output, relative humidity, temperature and land cover parameter AGR_5km_r in the urban background areas.

Table 4.17 Parameters of the linear regression models and of the ordinary kriging (nugget, sill, range) of PM_{2.5} annual average for 2015 in rural background and urban background areas for different mapping variants

Linear Regr. Model + OK of residuals	(C) Current 10x10		(C1) Like current 1x1		(L) LC included		(LT) LC incl., no ps. st.		(N) Without LC	
	rural	urb. b.	rural	urb. b.	rural	u. b.	rural	u. b.	rural	urb. b.
	coeff.	coeff.	coeff.	coeff.	coeff.	coeff.	coeff.	coeff.	coeff.	coeff.
c (constant)	1.24	1.65	1.36	1.68	1.46	7.99	9.53	8.49	8.55	8.77
a1 (EMEP model)	0.654	0.458	0.628	0.441	0.593	0.438	0.700	0.485	0.707	0.457
a2 (altitude_1km)	-0.0003		-0.0004		-0.0003		-0.0003		-0.0004	
a3 (altit._5km_r)										
a4 (wind speed)	-0.065		-0.073		-0.069					
a5 (rel. humidity)						-0.065	-0.087	-0.072	-0.077	-0.072
a6 (temperature)						-0.037		-0.032	-0.036	-0.035
a7 (s. solar rad.)							-0.046			
a8 (NAT_1km)					-0.0022		-0.0018			
a9 (AGR_5km_r)						0.0036		0.0040		
Adjusted R²	0.61	0.24	0.64	0.22	0.67	0.34	0.75	0.45	0.67	0.29
St. Err. [µg.m⁻³]	0.275	0.336	0.262	0.339	0.253	0.312	0.23	0.29	0.253	0.323
Nugget	0.047	0.018	0.038	0.021	0.034	0.024	0.024	0.023	0.034	0.021
Sill	0.076	0.099	0.065	0.099	0.059	0.087	0.045	0.065	0.061	0.092
Range [km]	1000	1000	1000	1000	1000	980	870	940	1000	1000

Note: Dark grey indicates variables not considered in the variant of the linear regression model. Light grey indicates variables not selected in the variant by the selecting procedure.

Comparison by cross-validation

Table 4.18 presents the mapping results of all variants for PM_{2.5} annual average, with their different sets of supplementary data that are mutually compared by means of the 'leave one out' cross-validation, for the rural and urban background areas.

Table 4.18 Comparison of different method variants of spatial interpolation showing RMSE, RRMSE, bias, R² and linear regression from the cross-validation scatter plots for PM_{2.5} annual mean in rural background (top) and urban background (bottom) areas, 2015. Units: µg.m⁻³ except RRMSE and R².

Spatial interpolation variant + supplementary data used		Rural background areas				
		RMSE	RRMSE	Bias	R ²	Regr. eq.
(C)	Current, 10x10 km (EMEP, altitude, wind speed)	2.5	21.9%	0.0	0.777	y = 0.764x + 2.6
(C1)	Like current, 1x1 km (EMEP, altitude, wind speed)	2.4	21.3%	-0.1	0.790	y = 0.767x + 2.6
(L)	Land cover included, 1x1 km (EMEP, altitude, wind speed, LC)	2.3	20.9%	0.0	0.799	y = 0.778x + 2.5
(LT)	LC included, no pseudo, 1x1 km (EMEP, alt., rel. hum., s. sol. rad., LC)	2.4	21.4%	0.1	0.796	y = 0.871x + 1.6
(N)	Without LC, 1x1 km (EMEP, altitude, rel. hum., temperature)	2.4	21.5%	0.0	0.786	y = 0.798x + 2.2
Spatial interpolation variant + supplementary data used		Urban background areas				
		RMSE	RRMSE	Bias	R ²	Regr. eq.
(C)	Current, 10x10 km (EMEP)	2.6	16.6%	0.1	0.821	y = 0.842x + 2.6
(C1)	Like current, 1x1 km (EMEP)	2.6	16.8%	0.2	0.816	y = 0.833x + 2.7
(L)	Land cover included, 1x1 km (EMEP, rel. hum., temperature, LC)	2.7	17.7%	0.1	0.797	y = 0.830x + 2.7
(LT)	LC included, no pseudo, 1x1 km (EMEP, rel. hum., temperature, LC)	3.0	19.2%	0.1	0.764	y = 0.827x + 2.8
(N)	Without LC, 1x1 km (EMEP, rel. hum., temperature)	2.6	17.1%	0.2	0.811	y = 0.833x + 2.7

One can see similar results as in the case of PM₁₀. The best results in the rural background areas are given by the variant (L), i.e. including land cover. This variant uses EMEP model, altitude, wind speed, and land cover class of natural areas as supplementary variables. Compared to the current methodology (C), one can see the improvement of the relative RMSE from 22 % to 21 %. The second best results in the rural background areas are given by the variant (C1), i.e. using EMEP model, altitude and wind speed as supplementary variables.

In the urban background areas, the best results are given for the variants (C) and (C1) using EMEP model only, with slightly better performance for the current method in 10x10 km². The same comments like in the case of the PM₁₀ mapping are valid, see Section 4.1.1.

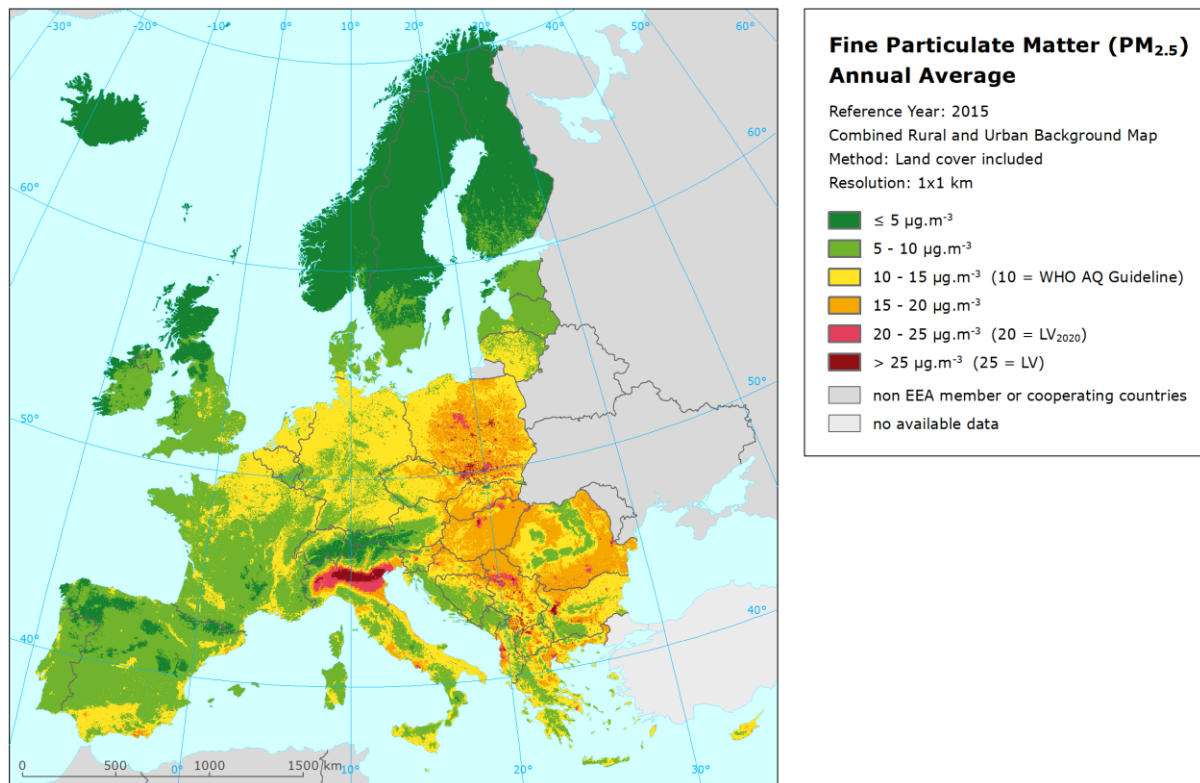
Conclusion

Based on the analysis results, it can be concluded that the inclusion of the land cover provides improvement on the PM_{2.5} mapping methodology in the rural areas. Therefore, it is recommended to implement this data source in the routine methodology. When introducing this, it is recommended to apply the 1x1 km² resolution from the very early process of mapping, i.e. from the creation of the separate map layers. For consistency reasons, it is recommended to do this change of resolution for both rural and urban background map layers. Thus, it is recommended to use the variant (L) for the rural map layer and the variant (C1) for the urban background map layer in the updated methodology.

Mapping results

Map 4.7 presents the rural and urban background merged map of PM_{2.5} annual average, created by the merge of rural and urban background map layers according to Equation 2.1. For the rural map layer, variant (L) is used. At limited areas with the lack of CLC2006 data (Andorra, Faroes, Jan Mayen), we substitute the estimated rural map layer value with the value of the variant (N). For the urban background layer, variant (C1) is used.

Map 4.7 Concentration map of PM_{2.5} annual average, rural and urban background merged map average using method with land cover data, 2015.



4.2.2 Traffic map layer inclusion

A similar approach as in the case of PM₁₀ was followed, again for the urban traffic areas only, as there are not enough representative rural traffic stations available for mapping. In order to see the level of the “urban traffic increment”, we compared the measurement data at the urban traffic stations with the underlying urban background map layer. In average, the urban traffic/background ratio is 1.12. This value is somewhat lower than in the case of PM₁₀ (see Section 4.1.1). However, the level of this ratio still justifies separately dealing with the urban traffic layer.

Like in the case of the rural and background areas, the pseudo PM_{2.5} stations are used. Their use in the traffic map layer creation is even more important than in the cases of rural and urban map layers, due to the lack of actual PM_{2.5} stations in some geographical areas. The linear regression relation for the estimates of pseudo PM_{2.5} data at locations of PM₁₀ stations with no PM_{2.5} measurement are calculated based on the data of the co-located PM₁₀ and PM_{2.5} urban traffic stations.

For the creation of the urban traffic map layer, we examined and mutually compared a similar set of mapping variants like for background areas. We have chosen as a baseline the variant (C1) using the same supplementary data as at the variant (C1) at the urban background mapping layer, i.e. EMEP model output. We apply the 1x1 km² resolution, we label this as (C1). Table 4.19 provides the overview of all the mutually compared variants.

Table 4.19 List of mutually compared variants of the mapping method, rural and urban background areas

Lab.	Variant Description	Area type	Grid resolution	EMEP	Alt.	Meteo	Popul. density	Land cover
(C1)	Like current UB, 1x1 km ²	Urban traffic	1x1 km ²	+	-	-	-	-
(L)	Land cover included	Urban traffic	1x1 km ²	+	- ^(a)	- ^(a)	- ^(a)	- ^(a)
(LT)	Land cover included, without pseudo PM _{2.5} stations	Urban traffic	1x1 km ²	+	- ^(a)	- ^(a)	- ^(a)	- ^(a)
(N)	Without land cover	Urban traffic	1x1 km ²	+	- ^(a)	- ^(a)	- ^(a)	-

(^a) Excluded in the backward stepwise selecting procedure

Table 4.20 presents for PM_{2.5} annual average the supplementary variables ultimately selected by the backward stepwise selection procedure and further applied, including their relevant statistical performance parameters at both the multiple linear regression and the subsequent interpolation by ordinary kriging of its residuals. It can be seen that apart from the EMEP model output, no additional supplementary data have been selected as significant performance contributors, leading to same results for variants (C1), (N) and (L), which we further call ‘optimal’.

Table 4.20 Parameters of the linear regression models and of the ordinary kriging (nugget, sill, range) of PM_{2.5} annual average for 2015 in urban traffic areas for different mapping variants

Linear Regr. Model + OK of its residuals	(C1) Like current 1x1	(L) LC included	(LT) LC incl., no pseudo st.	(N) Without LC
	urb. tr.	urb. tr.	urb. tr.	urb. tr.
	coeff.	coeff.	coeff.	coeff.
c (constant)	1.50	1.50	26.03	1.50
a1 (EMEP model)	0.505	0.505	0.526	0.505
a2 (altitude_1km)				
a3 (altit._5km_r)				
a4 (wind speed)				
a5 (NAT_1km)				
a6 (AGR_5km_r)				
Adjusted R²	0.54	0.54	0.55	0.54
St. Err. [µg.m⁻³]	0.262	0.262	0.25	0.262
Nugget	0.026	0.026	0.013	0.026
Sill	0.041	0.041	0.041	0.041
R	370	370	460	370

Note: Dark grey indicates variables not considered in the variant of the linear regression model. Light grey indicates variables not selected in the variant by the selecting procedure.

Comparison by cross-validation

Table 4.21 presents the mapping results of both variants, i.e. with and without the use of the pseudo PM_{2.5} stations, by means of the ‘leave one out’ cross-validation (Section 2.3), for the urban traffic areas.

Table 4.21 Comparison of different method variants of spatial interpolation showing RMSE, RRMSE, bias, R² and linear regression from the cross-validation scatter plots for PM_{2.5} annual mean in urban traffic areas, 2015. Units: µg.m⁻³ except RRMSE and R².

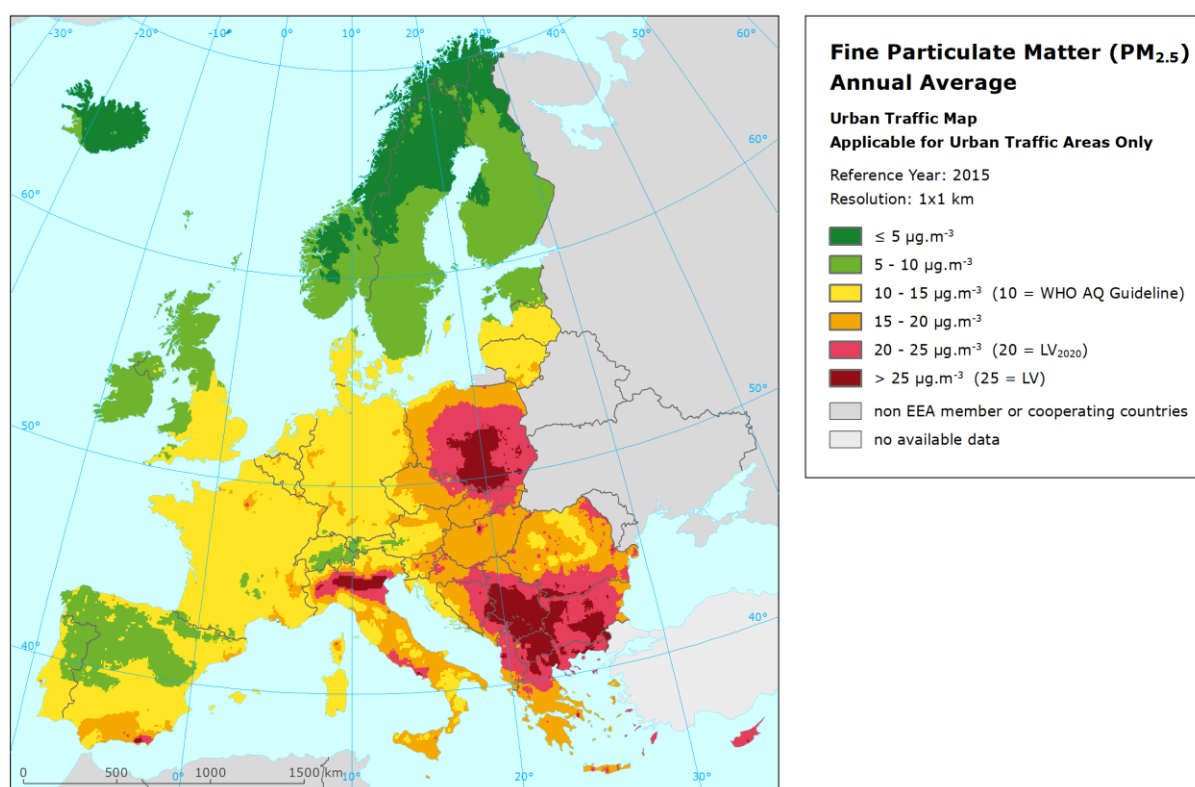
spatial interpolation variant + supplementary data used	Urban traffic areas				
	RMSE	RRMSE	Bias	R ²	Regr. eq.
(C1)=(N)=(L) Like current UB, 1x1 km (EMEP)	3.2	22.0%	-0.2	0.674	y = 0.617x + 5.5
(LT) No pseudo, 1x1 km (EMEP)	3.1	20.8%	-0.2	0.706	y = 0.708x + 4.1

The main message of Table 4.21 is that the relative RMSE of both methods is about 21-22 %. From this one can conclude that the traffic map layer gives quite reliable estimates for the urban traffic air quality and can be routinely applied. It can be seen that the variant (LT) without the pseudo PM_{2.5} station gives somewhat better results in the areas covered by the PM_{2.5} measurements. Nevertheless, due to the lack of the PM_{2.5} urban traffic stations in some geographical areas there is a need to use the pseudo PM_{2.5} stations.

Mapping results

Map 4.8 presents the urban traffic map layer for PM_{2.5} annual average for 2015. The map is applicable for urban traffic areas only.

Map 4.8 Concentration map of PM_{2.5} annual average, urban traffic air quality, 2015. Applicable for urban traffic areas only.



4.2.3 Final concentration map

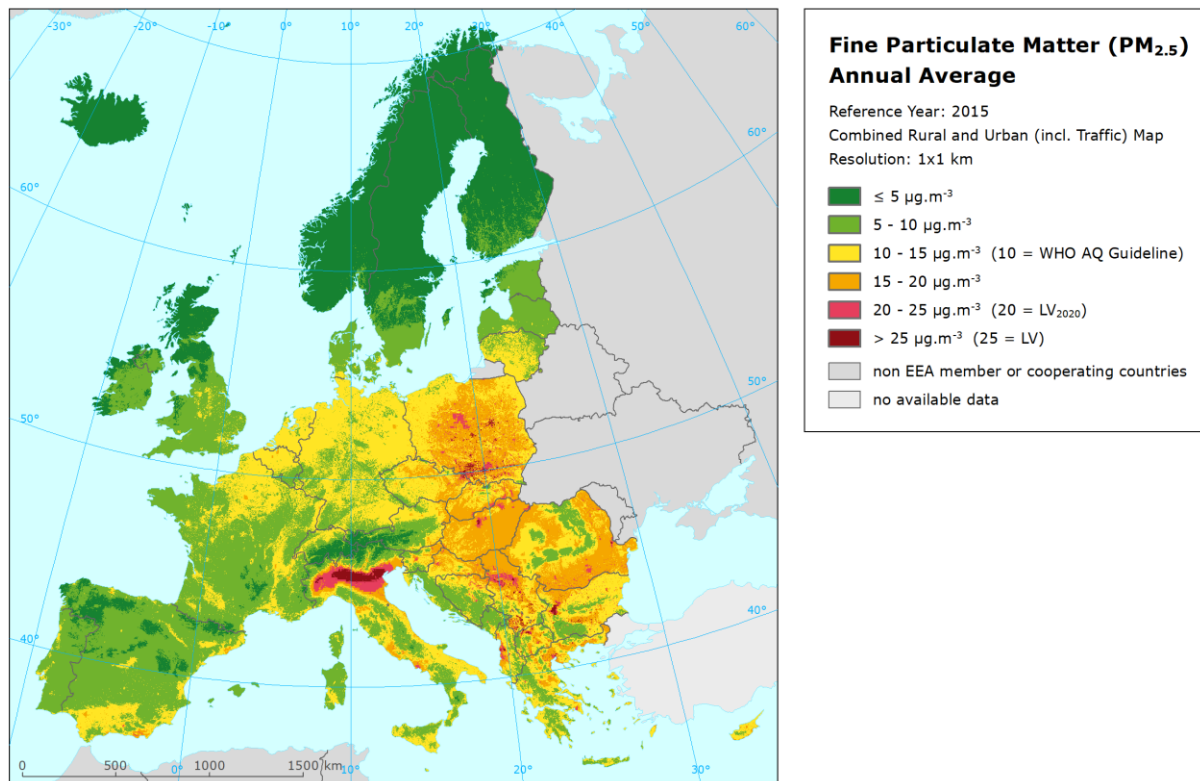
The traffic map layer as prepared in Section 4.2.2 has been integrated with the rural and urban background map as developed in Section 4.2.1, based on Equation 2.8. Like in the case of PM₁₀ (see Section 4.1.3), in the setting of the weight of the traffic map layer $w_T(i)$ (see Equations 2.7), a brief literature review on the spatial gradients of NO₂ and PM concentrations along the roads (see Annex) has been utilized, as well as a dispersion model exercise (Annex, A.3). This exercise shows that gradient of PM_{2.5} appears to be slightly less pronounced than for the other two pollutants. However, altogether it can be concluded that the spatial gradients between the pollutants are relatively similar over short distances. For this reason and for methodological consistency with PM₁₀ mapping, the similar weight of the traffic map layer like for PM₁₀ and NO₂ has been applied, following Equation 4.1.

Mapping results

Map 4.9 presents the final concentration map of PM_{2.5} annual average for 2015 created by including the traffic map layer as presented in Map 4.8 in the rural and urban background map of annual average as presented in Map 4.7.

In terms of mapping variants, (L) variant is used for the rural map layer, (C1) variant for the urban background, and (C1) = (L) = (N) variant for the urban traffic map layers. It is recommended to follow these variants in the routine PM_{2.5} mapping methodology.

Map 4.9 Concentration map of PM_{2.5} annual average of daily means using method with land cover included, 2015



Uncertainty estimates

Next to the cross-validation uncertainty estimates for the different mapping layers (see Tables 4.18 and 4.21, for the relevant map variants), a simple comparison between the point observation values and interpolated prediction values spatially averaged at 1x1 km² grid cells has been made, see Table 4.22.

Looking at the uncertainty grid prediction results for different map layers, similar results as for PM₁₀ are observed. One can see that both rural and urban background areas (represented by rural background resp. urban/suburban background stations) are well represented in both the background merged and the final merged maps. However, this is not true for the urban traffic areas, which are well represented only in the separate urban traffic map layer. It is clearly seen that not only in the background merged map (which is created without the use of the traffic map layer), but also in the final merged map, urban traffic areas are somewhat underestimated, though they are better represented than in the case of PM₁₀. The level of the underestimation is cc. 1 µg.m⁻³, i.e. smaller than for PM₁₀. The underestimation is caused by the 1x1 km² resolution of the maps, which is too coarse to distinguish the traffic urban air quality. This fact is needed to be taken into account in the exposure estimates (Section 4.2.4), i.e. the urban traffic areas should be dealt with separately in the exposure calculations.

Table 4.22 Statistical indicators from the scatter plots for the cross-validation scatter plots from separate (rural, urban background or urban traffic) map layers and for the predicted grid values from separate (rural, urban background or urban traffic) map layers, background merged map and final merged map versus the measurement point values for rural (upper left), urban background (upper right) and urban traffic (bottom left) stations for PM_{2.5} annual average 2015.

Map layer		rural background stations				
		RMSE	RRMSE	bias	R ²	lin. r. equation
(L)	cross-valid. prediction, separate rural background map layer	2.3	20.9%	0.0	0.799	y = 0.778x + 2.5
	grid prediction, 1x1 km ² , separate rural background map layer	2.0	18.2%	-0.2	0.853	y = 0.793x + 2.1
(r-ub merged)	grid prediction, 1x1 km ² , background merged map	2.2	19.3%	-0.1	0.829	y = 0.798x + 2.2
(r-ub-ut merged)	grid prediction, 1x1 km ² final merged map	2.2	19.3%	-0.1	0.829	y = 0.798x + 2.2
Map layer		urban/suburban background stations				
		RMSE	RRMSE	bias	R ²	lin r. equation
(C1)	cross-valid. prediction, separate urban background map layer	2.6	16.8%	0.2	0.816	y = 0.833x + 2.7
	grid prediction, 1x1 km ² separate urban background map layer	1.9	12.4%	-0.1	0.900	y = 0.868x + 2.0
(r-ub merged)	grid prediction, 1x1 km ² , background merged map	2.2	14.3%	-0.2	0.867	y = 0.840x + 2.3
(r-ub-ut merged)	grid prediction, 1x1 km ² final merged map	2.2	14.6%	-0.1	0.861	y = 0.830x + 2.5
Map layer		urban/suburban traffic stations				
		RMSE	RRMSE	bias	R ²	lin. r. equation
(C1) = (N) = (L)	cross-valid. prediction, separate urban traffic map layer	3.2	22.0%	-0.2	0.674	y = 0.617x + 5.5
	grid prediction, 1x1 km ² separate urban traffic map layer	2.4	16.2%	-0.1	0.832	y = 0.733x + 3.8
(r-ub merged)	grid prediction, 1x1 km ² , background merged map	3.0	20.4%	-1.5	0.790	y = 0.738x + 2.4
(r-ub-ut merged)	grid prediction, 1x1 km ² final merged map	2.9	19.5%	-1.3	0.800	y = 0.738x + 2.5

4.2.4 Exposure estimates

The population exposure estimates for PM_{2.5} annual average has been calculated similarly as for PM₁₀, i.e. using Equation 2.8, with the weight $w_T(i)$ calculated according to Equation 4.1.

Table 4.23 presents the final population exposure estimate of PM_{2.5} annual average for 2015, based on the method with land cover data and traffic map layer included. In this estimate, the rural and urban background annual average map as presented in Map 4.7 and the urban traffic map layer as presented in Map 4.8 are used.

Table 4.24 shows the comparison of the final exposure estimate for PM_{2.5} annual average for 2015 as presented in Table 4.23 with the exposure estimate calculated based on the rural and background merged map as presented in Map 4.7, as well as with the current approach (see Section 2.1) as presented in Horálek et al. (2018). In the current method, (C) variants of both rural and urban background map layers are applied. For all three methods, the percentage of population living above LV is presented, as well as the population-weighted concentration. The method presented in Table 4.20 (i.e. with the most realistic results) is marked by dark orange. The method presented in Map 4.7 is marked by light orange.

As for PM₁₀, the differences between “Background” and “Current” results are small, except for the highly polluted areas (Balkan). Comparing the “Final” and “Background” results, one can see the effect of the traffic map layer inclusion. This effect (i.e. increase of concentration levels) is smaller than for PM₁₀, what is in agreement with the discussion of Table 4.10. The reason is in the lower level of the traffic increment compared to PM₁₀.

As can be seen, the implementation of both land cover and traffic map layer inclusions leads into quite limited increase in the estimates of both the population-weighted concentration (cc. 0.2 µg.m⁻³) and the percentage population exposed to concentrations above LV (cc. 0.2 %) across Europe.

Table 4.23 Population exposure and population-weighted concentration using method with land cover data and traffic map layer included, PM_{2.5} annual average, 2015

Country	Population [inhbs . 1000]	PM _{2.5} annual average, exposed population [%]						Population weighted conc. [µg.m ⁻³]	
		< LV ₂₀₂₀				> LV ₂₀₂₀			
		< 5 µg.m ⁻³	5 - 10 µg.m ⁻³	10 - 15 µg.m ⁻³	15 - 20 µg.m ⁻³	20 - 25 µg.m ⁻³	> 25 µg.m ⁻³		
Albania	AL	2 892		0.7	10.2	23.2	41.1	24.8	20.9
Andorra	AD	78	0.2	10.5	89.3				12.8
Austria	AT	8 576	0.3	10.0	57.3	32.4			13.5
Belgium	BE	11 237		1.9	90.4	7.6			13.1
Bosnia & Herzegovina	BA	3 825		3.3	20.2	33.8	38.6	4.0	18.7
Bulgaria	BG	7 202		0.5	7.3	11.5	32.8	47.9	24.5
Croatia	HR	4 225		3.0	26.5	35.9	34.6		17.4
Cyprus	CY	1 173		0.2	12.1	79.3	8.2	0.3	17.6
Czechia	CZ	10 538		0.4	19.8	64.3	12.4	3.1	17.1
Denmark	DK	5 660	0.4	48.3	51.3				9.8
Estonia	EE	1 315	1.2	98.3	0.4				7.0
Finland	FI	5 472	24.6	75.4					5.5
France (metropolitan)	FR	64 344	0.0	17.8	70.2	10.8	1.1		12.1
Germany	DE	81 198	0.0	2.3	92.6	5.0	0.1		12.5
Greece	GR	10 858		1.0	23.3	25.4	33.5	16.9	19.8
Hungary	HU	9 856			0.5	72.3	18.6	8.7	19.4
Iceland	IS	329	36.3	59.9	3.6	0.2			5.8
Ireland	IE	4 629	6.6	92.2	1.2				6.8
Italy	IT	60 796	0.0	2.9	26.6	36.3	17.5	16.7	18.5
Latvia	LV	1 986	0.0	41.3	44.9	12.8	1.0		11.3
Liechtenstein	LI	37	0.1	8.2	91.7				11.1
Lithuania	LT	2 921		4.1	92.6	3.3			12.4
Luxembourg	LU	563		5.7	87.2	7.1			12.3
Malta	MT	429		0.6	89.2	10			13.2
Monaco	MC	38			78.5	22			14.7
Montenegro	ME	622		7.0	13.0	53.5	18.3	8.2	18.9
Netherlands	NL	16 901		0.3	99.7	0.0			12.4
North Macedonia	MK	2 069		0.1	1.2	3.2	12.6	82.9	28.9
Norway	NO	5 166	36.2	62.8	1.0				5.9
Poland	PL	38 006		0.0	8.7	30.6	30.5	30.1	21.7
Portugal (excl. Az., Mad.)	PT	9 870	0.2	48.5	44.7	5.9	0.8		10.4
Romania	RO	19 871		0.3	15.8	53.2	30.0	0.7	18.2
San Marino	SM	33			14.3	86			16.1
Serbia (incl. Kosovo*)	RS	8 919		0.2	3.1	19.3	36.0	41.3	24.2
Slovakia	SK	5 421		0.0	1.9	63.8	33.2	1.1	19.2
Slovenia	SI	2 063		1.6	23.3	47.6	27.6		17.4
Spain (excl. Canarias)	ES	44 323	0.4	19.6	52.2	27.1	0.7	0.0	12.8
Sweden	SE	9 747	42.8	53.7	3.4				5.9
Switzerland	CH	8 238	0.6	11.2	83.3	4.9	0.0		12.0
United Kingdom (& dep.)	UK	64 875	0.8	56.3	42.8	0.0			9.6
Total	536 303		1.6	16.7	47.1	18.9	9.2	6.5	14.3
			18.3				15.7		
EU-28	504 055		1.3	16.8	48.5	19.2	8.5	5.7	14.1
			18.1				14.2		

Kosovo*	KS	1 805		0.1	3.4	9.8	13.2	73.5	27.2
Serbia (excl. Kosovo*)	RS	7 114		0.2	3.0	21.7	41.6	33.5	23.5

*) under the UN Security Council Resolution 1244/99

Note 1: Turkey is not included in the calculation due to the lack of air quality data.

Note 2: The percentage value "0.0" indicates that an exposed population exists, but it is small and estimated lesser than 0.05 %. Empty cells mean: no population in exposure.

As can be seen in Table 4.23 and in Horálek et al. (2018), according to the "Final" resp. "Current" results, 5.7 % resp. 5.5 % of the EU-28 population has been exposed to annual average concentrations above the limit value. According to EEA CSI004 (EEA, 2017b), about 7 % of the urban population in the EU-28 was exposed to PM_{2.5} concentrations above the limit value in 2015. The difference with the above mentioned

numbers is because the EEA accounts for the urban population in the larger agglomerations only (as far as measurements are available). Whereas, those maps presented here provide estimates for the total population, including the population in rural areas, smaller cities and villages. When it comes to the WHO AQ guideline, the urban population exposed to concentrations above its recommended value ($10 \mu\text{g}\cdot\text{m}^{-3}$) in 2015 was estimated at 83 %, which is more in line with the total population estimation of 82 % resp. 81 % as presented in Table 4.23 resp. Horálek et al. (2018).

Table 4.24 Population exposure above LV (left) and population-weighted concentration (right) using current method, method with land cover data included (Map 4.1) and method with LC data and traffic map layer included (Table 4.23), and differences between two methods, $\text{PM}_{2.5}$ annual average, 2015.

Country		Exposed population > LV [%]					Population-weighted concentration [$\mu\text{g}\cdot\text{m}^{-3}$]				
		Current TP'17/7	Backgr. M. 4.7	Differ. Back. -C.	Final T. 4.23	Differ. Fin.-Back.	Current TP'17/7	Backgr. M. 4.7	Differ. Back. -C.	Final T. 4.23	Differ. Fin.-Back.
Albania	AL	12.0	24.7	12.8	24.8	0.1	20.5	20.9	0.4	20.9	0.0
Andorra	AD	0	0	0	0	0	13.3	12.8	-0.5	12.8	0.0
Austria	AT	0	0	0	0	0	13.3	13.4	0.1	13.5	0.1
Belgium	BE	0	0	0	0	0	13.0	13.0	0.0	13.1	0.1
Bosnia & Herzegovina	BA	8.3	4.0	-4.3	4.0	0.0	18.9	18.7	-0.2	18.7	0.0
Bulgaria	BG	44.0	47.8	3.8	47.9	0.1	24.1	24.5	0.4	24.5	0.0
Croatia	HR	0	0	0	0	0.0	17.4	17.4	0.0	17.4	0.0
Cyprus	CY	0	0	0	0.3	0.3	16.9	17.1	0.2	17.6	0.5
Czechia	CZ	3.1	3.1	0.0	3.1	0.0	17.0	17.1	0.0	17.1	0.0
Denmark	DK	0	0	0	0	0	9.7	9.8	0.1	9.8	0.1
Estonia	EE	0	0	0	0	0	6.7	6.9	0.2	7.0	0.1
Finland	FI	0	0	0	0	0	5.3	5.4	0.1	5.5	0.0
France (metropolitan)	FR	0	0	0	0	0	11.9	11.9	0.1	12.1	0.2
Germany	DE	0	0	0	0	0	12.3	12.4	0.1	12.5	0.1
Greece	GR	16.6	14.6	-2.0	16.9	2.2	19.1	19.6	0.5	19.8	0.2
Hungary	HU	0.0	8.6	8.6	8.7	0.0	18.9	19.4	0.4	19.4	0.0
Iceland	IS	0	0	0	0	0	5.5	5.6	0.1	5.8	0.2
Ireland	IE	0	0	0	0	0	6.5	6.7	0.2	6.8	0.1
Italy	IT	17.4	16.4	-1.0	16.7	0.3	18.5	18.4	0.0	18.5	0.1
Latvia	LV	0	0	0	0	0.0	10.6	11.1	0.5	11.3	0.2
Liechtenstein	LI	0	0	0	0	0	11.0	11.1	0.2	11.1	0.0
Lithuania	LT	0	0	0	0	0	11.7	12.2	0.5	12.4	0.2
Luxembourg	LU	0	0	0	0	0	12.0	12.0	0.0	12.3	0.3
Malta	MT	0	0	0	0	0	12.8	12.8	-0.1	13.2	0.4
Monaco	MC	0	0	0	0	0	14.4	14.4	0.0	14.7	0.3
Montenegro	ME	9.9	8.2	-1.7	8.2	0.0	18.5	18.9	0.3	18.9	0.0
Netherlands	NL	0	0	0	0	0	12.3	12.4	0.1	12.4	0.1
North Macedonia	MK	78.8	82.8	4.1	82.9	0.0	28.7	28.9	0.2	28.9	0.0
Norway	NO	0	0	0	0	0	5.9	5.9	0.0	5.9	0.0
Poland	PL	30.3	30.0	-0.3	30.1	0.1	21.6	21.7	0.1	21.7	0.0
Portugal (excl. Az., Mad.)	PT	0	0	0	0	0	9.8	10.2	0.4	10.4	0.2
Romania	RO	0.6	0.6	0.0	0.7	0.1	18.1	18.1	0.0	18.2	0.1
San Marino	SM	0	0	0	0	0	16.2	16.1	-0.1	16.1	0.0
Serbia (incl. Kosovo*)	RS	41.4	41.3	-0.1	41.3	0.1	23.9	24.2	0.3	24.2	0.0
Slovakia	SK	1.0	1.1	0.1	1.1	0.0	19.1	19.2	0.1	19.2	0.0
Slovenia	SI	0	0	0	0	0	17.4	17.4	0.0	17.4	0.0
Spain (excl. Canarias)	ES	0	0.0	0.0	0.0	0.0	12.7	12.7	0.0	12.8	0.1
Sweden	SE	0	0	0	0	0	5.9	5.8	-0.1	5.9	0.1
Switzerland	CH	0	0	0	0	0	11.8	11.9	0.1	12.0	0.1
United Kingdom (& dep.)	UK	0	0	0	0	0	9.4	9.4	0.0	9.6	0.1
Total		6.3	6.4	0.1	6.5	0.1	14.2	14.2	0.1	14.3	0.1
EU-28		5.5	5.6	0.0	5.7	0.1	14.0	14.1	0.1	14.1	0.1
Kosovo*	KS	11.9	73.5	61.6	73.5	0.0	26.4	27.2	0.8	27.2	0.0
Serbia (excl. Kosovo*)	RS	39.0	33.4	-5.6	33.5	0.1	23.3	23.5	0.1	23.5	0.0

*) under the UN Security Council Resolution 1244/99

Note 1: Turkey is not included in the calculation due to the lack of air quality data.

Note 2: The percentage value "0.0" indicates that an exposed population exists, but it is small and estimated lesser than 0.05 %. The percentage value "0" mean: no population in exposure.

5 Conclusion

For both PM₁₀ and PM_{2.5} mapping, the inclusion of CLC land cover data in the rural and urban background map creation has been examined, as well as the inclusion of the traffic map layer in the final merged map. In all steps of the mapping process, the 1x1 km² resolution has been applied. This mapping methodology is in agreement with the NO₂ mapping as developed in Horálek et al. (2017) and applied in Horálek et al. (2018a). The analysis has been done for PM₁₀ indicators annual average and 90.4 percentile of daily means and for PM_{2.5} annual average.

Land cover inclusion

Based on the analysis results, it can be concluded that the inclusion of the land cover provides improvement on both the PM₁₀ and PM_{2.5} mapping methodology in the rural areas. Therefore, it is recommended to implement this supplementary data sources in the routine methodology to calculate the rural background map layer. When introducing this, it is recommended to also move the application of the 1x1 km² resolution to its earliest stage of the 'regression – kriging – merging' mapping process, i.e. moving it from the combined final merging process-step to the early process-step of the regression and kriging stage when creating each separate rural and urban background map layer. It is recommended to do this change of resolution for both rural and urban background map layers to assure methodological consistency at all map layers.

Traffic map layer inclusion

Based on the urban and suburban traffic stations and suitable supplementary data, traffic map layers have been constructed for all examined PM₁₀ and PM_{2.5} indicators. These map layers apply as such on urban areas only, since an interpolated rural traffic map layer cannot be constructed due to the lack of rural traffic stations. The uncertainty cross-validation results of these traffic map layers in terms of the relative RMSE are satisfactory, being 20 %, 26 % and 22 % respectively (for the PM₁₀ indicators annual average and the 90.4 percentile of daily means and for the PM_{2.5} annual average). Leading from this, one can conclude that the traffic map layers give quite reliable estimates for the urban traffic air quality for all examined PM₁₀ and PM_{2.5} indicators. Thus, the inclusion of the traffic map layers in the routine PM mapping methodology can be recommended.

The merge of the background and the traffic map layers, which is based on the buffers around the roads, was examined. Overall, based on the literature review and a dispersion modelling exercise, it seems to be an appropriate assumption that the horizontal spatial gradient as a function of distance from a major road is relatively similar for both NO₂ and PM₁₀, however the gradient of PM_{2.5} appears to be slightly less pronounced than for the other two pollutants. It is a fair assumption for the purposes of the ETC/ACM mapping tasks, which primarily only considers a distance of maximum 50–75 m from the road, that the horizontal spatial gradients between the pollutants are relatively similar over such short distances. Based on this conclusion, the use of the similar weighting process of the background and the traffic map layers like for NO₂ can be recommended.

For all the examined PM indicators, the traffic map layer has been incorporated with the background map into the final merged map, using the described weighting procedure. In this final merged map, the rural and urban background areas are well represented, while the urban traffic areas are somewhat underestimated, due to the 1x1 km² resolution of the map. This is acceptable for the map itself (due to the chosen resolution). However, this final 1x1 km² map would not be suitable for the population exposure calculations. Therefore, it is recommended to apply for the population exposure calculations the similar approach like for NO₂, i.e. the approach based on separately dealing with the background and the urban traffic map layers. This recommendation applies for all PM indicators.

References

- Beelen R, Hoek G, Pebesma E, Vienneau D, de Hoogh K, Briggs D, 2009. Mapping of background air pollution at a fine spatial scale across the European Union. *Science of the Total Environment* 407, 1852–1867. doi:10.1016/j.scitotenv.2008.11.048
- Beelen R, Hoek G, Vienneau D, Eeftens M et al., 2013. Development of NO₂ and NO_x land use regression models for estimating air pollution exposure in 36 study areas in Europe – The ESCAPE project. *Atmospheric Environment* 72, 10–23.
- CHMI, 2017. Air Pollution and Atmospheric Deposition in Data, the Czech Republic. Available at: http://portal.chmi.cz/files/portal/docs/uoco/isko/tab_roc/tab_roc_en.html Accessed 24/11/17
- Danielson JJ, Gesch DB, 2011. Global multi-resolution terrain elevation data 2010 (GMTED2010): U.S. Geological Survey Open-File Report 2011–1073. Available at: <https://lta.cr.usgs.gov/GMTED2010> Accessed 24/11/17
- Denby B, Gola G, De Leeuw F, De Smet P, Horálek J, 2011. Calculation of pseudo PM_{2.5} annual mean concentrations in Europe based on annual mean PM₁₀ concentrations and other supplementary data. ETC/ACC Technical Paper 2010/9. http://acm.eionet.europa.eu/reports/ETCACC_TP_2010_9_pseudo_PM2.5_stations Accessed 1/10/18
- EEA, 2011. Guide for EEA map layout. EEA operational guidelines. August 2011, version 4. Available at: http://www.eionet.europa.eu/gis/docs/GISguide_v4_EEA_Layout_for_map_production.pdf Accessed 24/11/17
- EEA, 2017a. Air Quality e-Reporting. Air quality database. Available at: <http://www.eea.europa.eu/data-and-maps/data/aqereporting-2> Accessed 24/11/17
- EEA, 2017b. Exceedance of air quality limit values in urban areas. CSI004 indicator assessment. <https://www.eea.europa.eu/data-and-maps/indicators/exceedance-of-air-quality-limit-3/assessment-3>
- ECMWF, 2017. Meteorological Archival and Retrieval System (MARS). Available at: <http://www.ecmwf.int/> Accessed 1/3/17
- EMEP, 2017. Transboundary particular matter, photo-oxidants, acidifying and eutrophying components. EMEP Report 1/2017. Available at: http://emep.int/publ/reports/2017/EMEP_Status_Report_1_2017.pdf Accessed 24/11/17
- Hoek G, Beelen R, de Hoogh K, Vienneau D, Gulliver J, P. Fischer, and D. Briggs, 2008. A review of land-use regression models to assess spatial variation of outdoor air pollution, *Atmos. Environ.*, 42(33), 7561–7578, doi:10.1016/j.atmosenv.2008.05.057.
- Horálek J, Denby B, de Smet P, de Leeuw F, Kurfürst P, Swart R, van Noije T, 2007. Spatial mapping of air quality for European scale assessment. ETC/ACC Technical paper 2006/6. Available at: http://acm.eionet.europa.eu/reports/ETCACC_TechnPaper_2006_6_Spat_AQ Accessed 24/11/17 Accessed 1/10/18
- Horálek J, de Smet P, de Leeuw F, Coňková M, Denby B, Kurfürst P, 2010. Methodological improvements on interpolating European air quality maps. ETC/ACC Technical Paper 2009/16. Available at: http://acm.eionet.europa.eu/reports/ETCACC_TP_2009_16_Improv_SpatAQmapping Accessed 1/10/18

Horálek J, de Smet P, Schneider P, Kurfürst P, de Leeuw F, 2017. Inclusion of land cover and traffic data in NO₂ mapping methodology. ETC/ACM Technical Paper 2016/12. Available at: http://acm.eionet.europa.eu/reports/ETCACM_TP_2016_12_LC_and_traffic_data_in_NO2_mapping

Horálek J, de Smet P, de Leeuw F, Kurfürst P, Benešová N, 2018a. European air quality maps for 2015. ETC/ACM Technical Paper 2017/7. Available at: http://acm.eionet.europa.eu/reports/ETCACM_TP_2017_7_AQMaps2015 Accessed 1/10/18

Horálek J, de Smet P, Schneider P, Maiheu B, de Leeuw F, Janssen S, Benešová N, Lefebvre W, 2018b. Satellite data inclusion and kernel based potential improvements in NO₂ mapping. ETC/ACM Technical Paper 2017/14. Available at: http://acm.eionet.europa.eu/reports/ETCACM_TP_2017_14_Improved_AQ_NO2mapping Accessed 1/10/18

JRC, 2009. Population density disaggregated with Corine land cover 2000. 100x100 m grid resolution, EEA version popu01clcv5.tif of 24 Sep 2009. Available at: <http://www.eea.europa.eu/data-and-maps/data/population-density-disaggregated-with-corine-land-cover-2000-2> Accessed 24/11/17

Mareckova K, Pinterits M, Ullrich B, Wankmüller R, Mandl N, 2017. Inventory Review 2017. Review of emission data reported under the LRTAP Convention and NEC Directive. Stage 1 and 2 review & Status of gridded and LPS data. EEA/CEIP Technical Report 2/2017. Available at: http://www.ceip.at/fileadmin/inhalte/emep/pdf/2017/InventoryReport_2017_v3.pdf Accessed 24/11/17

Meijer JR, Huijbregts MAJ, Schotten CGJ, Schipper AM, 2018. Global patterns of current and future road infrastructure. *Environmental Research Letters* 13 0640, <https://doi.org/10.1088/1748-9326/aabd42>

NILU, 2017. EBAS, database of atmospheric chemical composition and physical properties. Available at: <http://ebas.nilu.no/> Accessed 24/11/17

ORNL, 2008. ORNL LandScan high resolution global population data set. Available at: http://www.ornl.gov/sci/landscan/landscan_documentation.shtml Accessed 24/11/17

PBL (2018). GRIP: Global Road Inventory Project (GRIP). Available at: http://geoservice.pbl.nl/website/flexviewer/index.html?config=PBL_GRIP.xml¢er=556597,6800125&scale=5000000

Simpson D, Benedictow A, Berge H, Bergström R, Emberson LD, Fagerli H, Hayman GD, Gauss M, Jonson JE, Jenkin ME, Nyíri A, Richter C, Semeena VS, Tsyro S, Tuovinen J-P, Valdebenito A, Wind P, 2012. The EMEP MSC-W chemical transport model – technical description. *Atmospheric Chemistry and Physics*, 12, 7825–7865, doi:10.5194/acp-12-7825-2012. <http://www.atmos-chem-phys.net/12/7825/2012/acp-12-7825-2012.html> Accessed 24/11/17

WHO, 2005. WHO Air quality guidelines for particulate matters, ozone, nitrogen dioxide and sulphur dioxide. Global update 2005. http://www.who.int/phe/health_topics/outdoorair/outdoorair_agg/en/index.html

Annex – On the spatial gradient of NO₂ and PM along roads

A.1 Introduction and Motivation

The spatial gradient of the concentrations of nitrogen dioxide (NO₂) and particulate matter (PM) as a function of horizontal distance from roads constitutes important information for a wide variety of applications in air quality mapping. This includes applications such as for land-use regression modelling (LUR) (Beelen et al., 2013) or within the air quality mapping carried out operationally within the framework of the ETC/ACM (Horálek et al., 2018). We provide here a short overview of some existing scientific literature on the subject and show some results of an experiment with the Norwegian urban air quality model EPISODE to provide some information on the typical model-based spatial gradient from roads for both NO₂ and PM.

A.2 Brief Literature Overview

Quite a few studies have been published in the scientific literature that directly or indirectly investigate the spatial gradient of air pollutants from roads. In the following we present an entirely non-exhaustive list of publications along these lines:

Gilbert et al. (2003) used passive sampling devices to study the spatial variation of ambient nitrogen dioxide (NO₂) with increasing distance from a major highway. For distances between 0 m and 1310 m, they found that the NO₂ concentrations varied between 11.9 ppb and 29.3 ppb and that they decrease significantly with increasing logarithmic distance from the road (see Figure A.1).

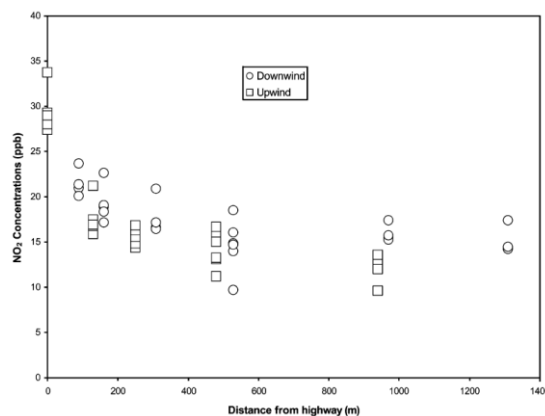


Figure A.1 - NO₂ concentration measured using passive sampling devices over the course of 1 week in Montreal as a function of distance from a major highway (Gilbert et al., 2003).

Pleijel et al., (2004) carried out a similar study in Sweden in which they distributed passive samplers at distances from around 10 m to ca. 300 m from a major highway. They found a logarithmic relationship. The slope of the regression was somewhat steeper in this study than in the one previously mentioned (Gilbert et al., 2003). This could possibly be related to the difference in landscape roughness, wind speed, atmospheric stability, and background ozone concentrations, although landscape roughness seems to be the least likely explanation given the relatively flat terrain of the study site in Sweden.

Allen et al., (2009) reported on an experiment in which they used passive samplers at 105 locations to study spatial gradients of the concentrations of various pollutants and noise as a function of distance from road. The study was carried out in Chicago and Riverside Country in the United States (see Figure A.2). They found that logarithmic distances to nearby major roads were moderately correlated with NO₂. They also conclude that there is a moderate correlation between traffic noise and air pollution and as such there

is the potential for confounded results if noise and air pollution are not accurately assessed in epidemiological studies.

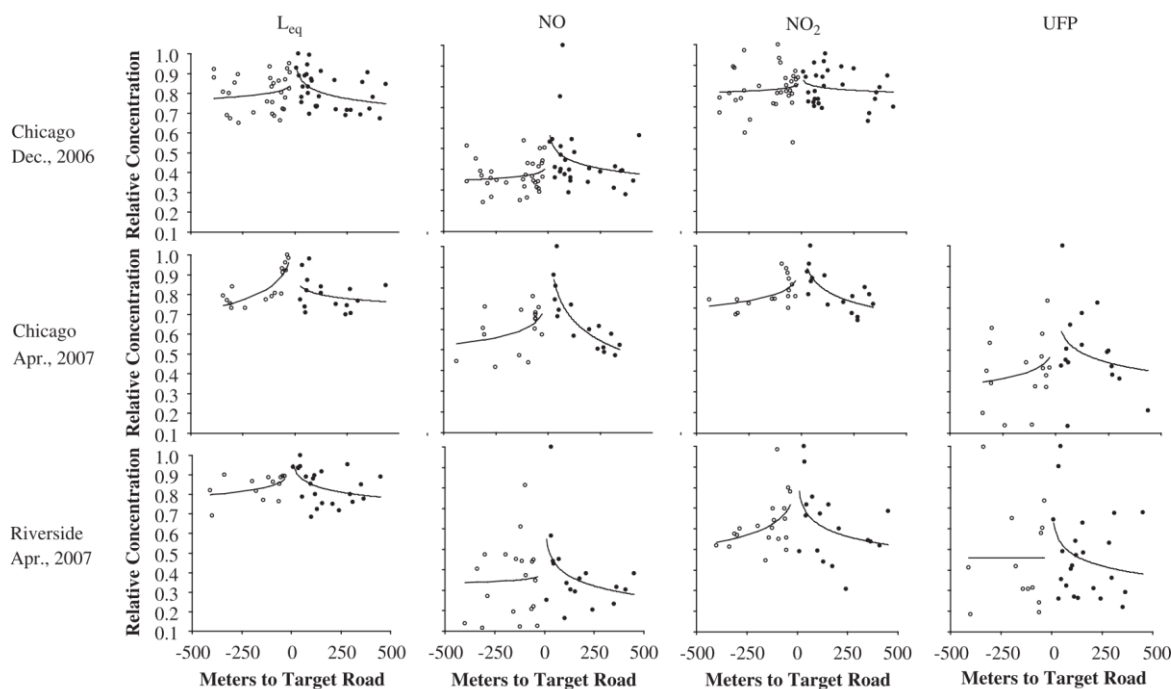


Figure A.2 - Concentration of air pollutants as a function of distance from a major roadway, both for upwind and downwind data, including logarithmic functions fitted to the data (Allen et al., 2009). L_{eq} stands for 5-min A-weighted equivalent continuous sound pressure levels, UFP stands for ultrafine particles.

Gonzales et al., (2005) used passive samples for NO_2 at 20 sites and four air quality monitoring stations to study the gradient of NO_2 concentrations in El Paso, Texas. They found average concentrations ranging from 11 to 37.5 ppb over a 7-day period. They further found that the site elevation and the distance to a main highway explained 81% of the variance and conclude that proximity to vehicle-related source of NO_2 and site elevation are the key predictors.

While there has been quite some work on roadside gradients of NO_2 , significantly less literature has been published on the spatial gradient of PM along roads. However, several studies look at changes in particle number with distance from the road. One example is the study of Massoli et al. (2012) who provided measurements of particle number as a function of the distance from a major highway (the Long Island Expressway) using a mobile laboratory. They found a significant reduction in particle number with distance, but do not provide measurements of PM mass.

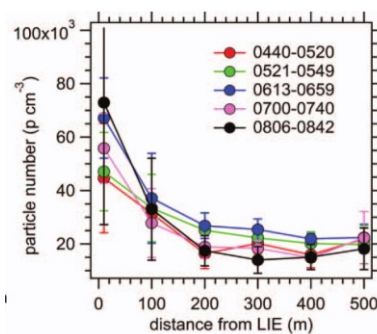


Figure A.3 - The number of particles measured using a mobile laboratory, as a function of distance from the Long Island Expressway (LIE) (Massoli et al., 2012)

McAdam et al., (2011) reported no clear distance decay pattern for PM_{2.5}, however they only made measurements at 3 distances from the road (10 m, 30 m, and 60 m).

Hitchins et al., (2000) give an overview of their study of measuring number concentrations of particles from vehicle emissions at increasing distance from a major road. They found that the concentration of fine and ultrafine particles decays to approximately half the maximum at a distance of approximately 100-150 m from the road, when the wind is blowing from the road. With the wind parallel to the road this reduction to half the concentration occurs at approximately 50-100 m. More specifically for PM_{2.5}, they found that PM_{2.5} levels decrease with distance, namely at a distance of 375 m to 75% of the maximum for wind from the road and to 65% with the wind parallel to the road (see Figure A.4).

Hagler et al. (2009) measured the number of ultrafine particles as a function of distance from a roadway and found a strong exponentially decreasing horizontal spatial gradient. They also compared other similar studies and report that all such experiments appear to exhibit a general exponential decay with increasing distance from the road, but that the rate of decrease varies from study to study. This could be related to background levels at each site, meteorological conditions, and differences in sampling techniques (see Figures A.5 and A.6).

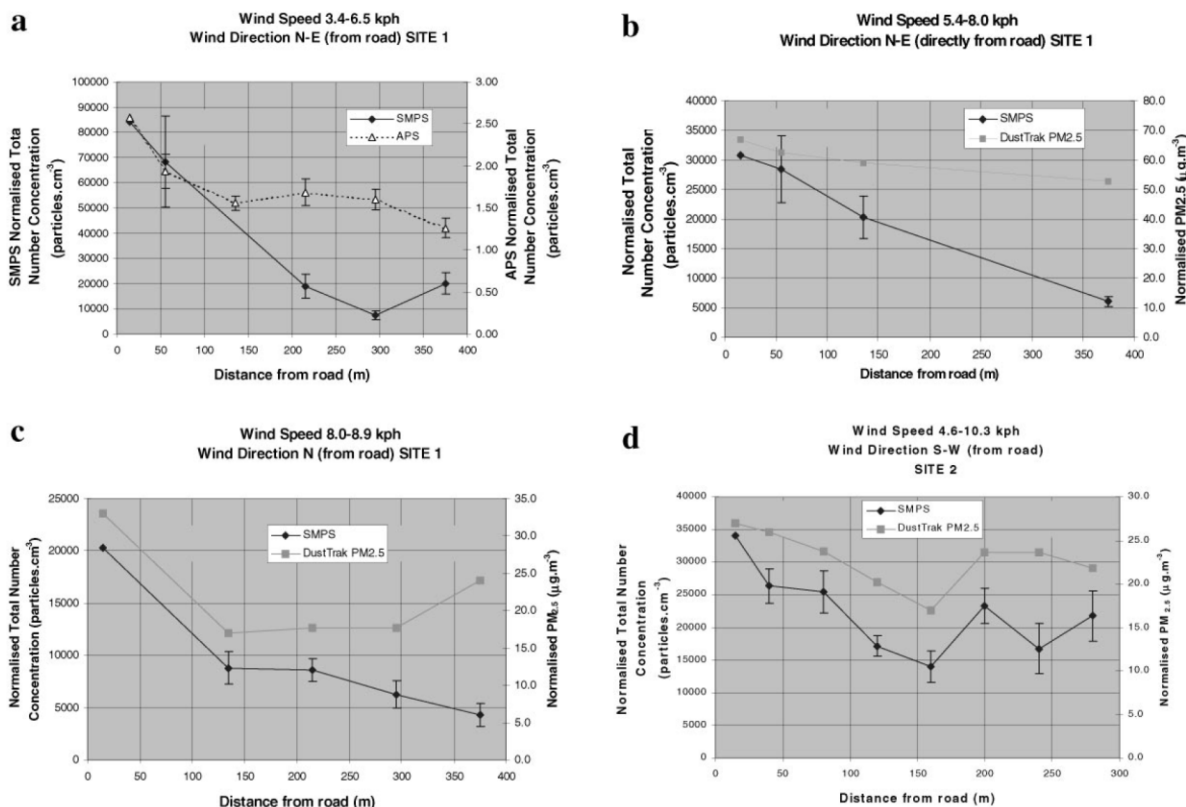


Figure A.4 - Horizontal spatial gradients in the concentrations of submicrometre particulate matter with wind direction from the road (Hitchins et al., 2000).

Finally Karner et al. (2010) provided a good overview of the road spatial gradients from various studies. Synthesizing the results of 41 experimental studies published between 1978 and 2008 they concluded that almost all pollutants decay to their background levels by 160-570 m from the edge of a road.

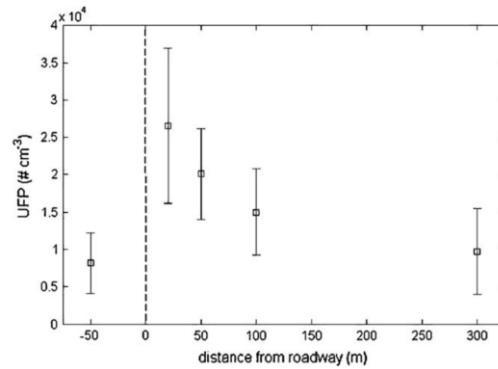


Figure A.5 - Number of ultrafine particles measured as a function of distance from a roadway (Hagler et al., 2009)

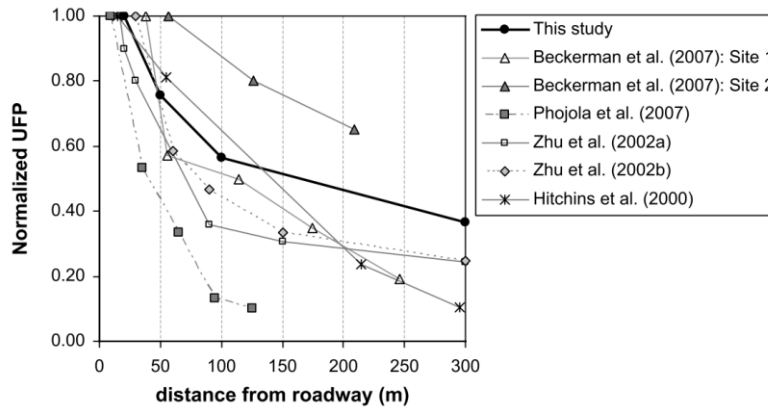


Figure A.6 - Comparison of the spatial gradient of ultrafine particles reported by various studies (Hagler et al., 2009)

A.3 Results from an experiment using the dispersion model EPISODE

In addition to the literature review, we carried out a small experiment to extract the typical horizontal spatial gradient from roads as it is physically (not statistically) modeled by the Norwegian urban air quality dispersion model EPISODE. The EPISODE model (Slørddal et al., 2003) is a 3-D Eulerian/Lagrangian dispersion model that provides urban- and regional-scale air quality forecasts of atmospheric pollutants. The following description of EPISODE is taken from (Schneider et al., 2017): the model combines a Eulerian grid model with embedded subgrid models for computing the various pollutant concentrations that result from area-, point-, and line-based emission sources. Applying finite difference numerical methods, EPISODE integrates forward in time and solves the time-dependent advection and diffusion equation on a three-dimensional grid. EPISODE provides schemes for advection, turbulence, deposition, and chemistry, although the latter was not activated here for reasons of computational performance.

EPISODE contains a sub-grid line source model based on a standard integrated Gaussian model (Petersen, 1980), which computes the concentration levels of non-reactive pollutants from road traffic over distances up to hundreds of meters downwind. Most commonly, EPISODE is used for modeling airborne species such as NO₂, NO_x, PM₁₀, PM_{2.5}, CO, and SO₂. Validation studies have shown good correspondence between modeled and measured concentrations of NO₂, PM₁₀, and PM_{2.5} (Ofstedal et al., 2009).

Figure A.7 shows example outputs for annual average concentrations of NO₂, PM₁₀, and PM_{2.5} over the Oslo area. Already in these maps the typical spatial gradient as produced by the model can be observed. In order to highlight this a little better, we show in Figure A.8 a small area in the south-eastern corner of the model domain that includes a major 4-lane highway and otherwise to the east of the highway primarily open flat terrain. The spatial gradients seen here can thus be considered fairly typical for the output of EPISODE when averaged over long periods. Finally, Figure A.9 shows the extracted concentration values along the transect indicated in Figure A.8 and as such present the typical spatial gradient for the three

pollutants in this area. In order to eliminate the effect of the different overall concentration levels for the three pollutants, the data was normalized by the concentration level at the road (Figure A.9 bottom panel).

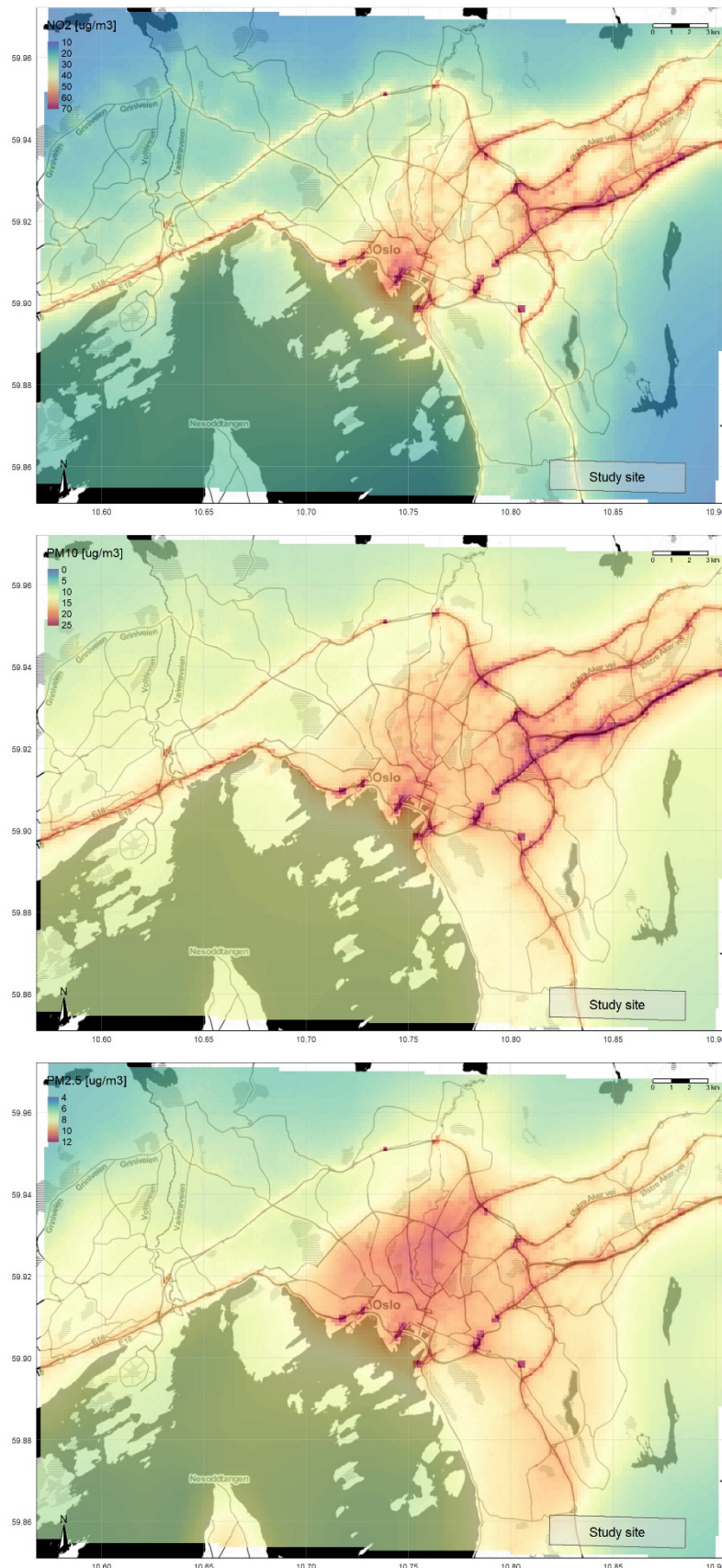


Figure A.7: Comparison of annual average maps of NO_2 (top), PM_{10} (middle), and $\text{PM}_{2.5}$ (bottom) over the greater Oslo area as produced by the EPISODE dispersion model. In the southeast corner the area of the study site for the gradients is shown.

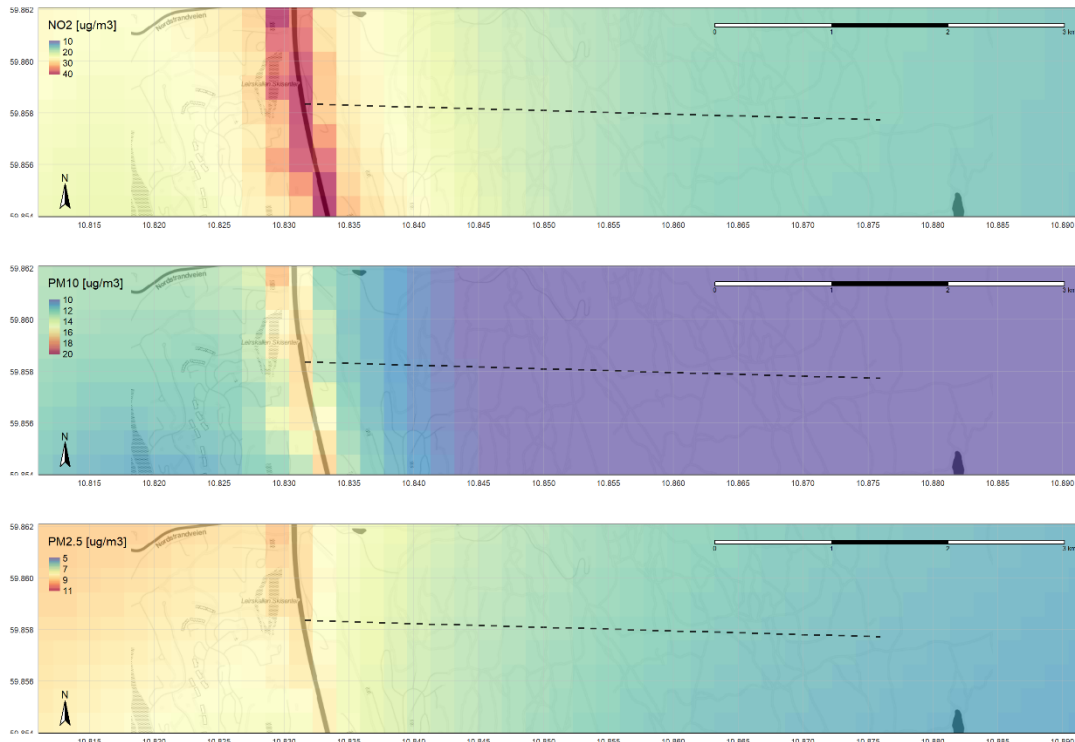


Figure A.8: Spatial gradient of NO₂ (top), PM₁₀ (middle), and PM_{2.5} as modelled by the EPISODE dispersion model. The dashed line indicates the line along which values were extracted for comparison.

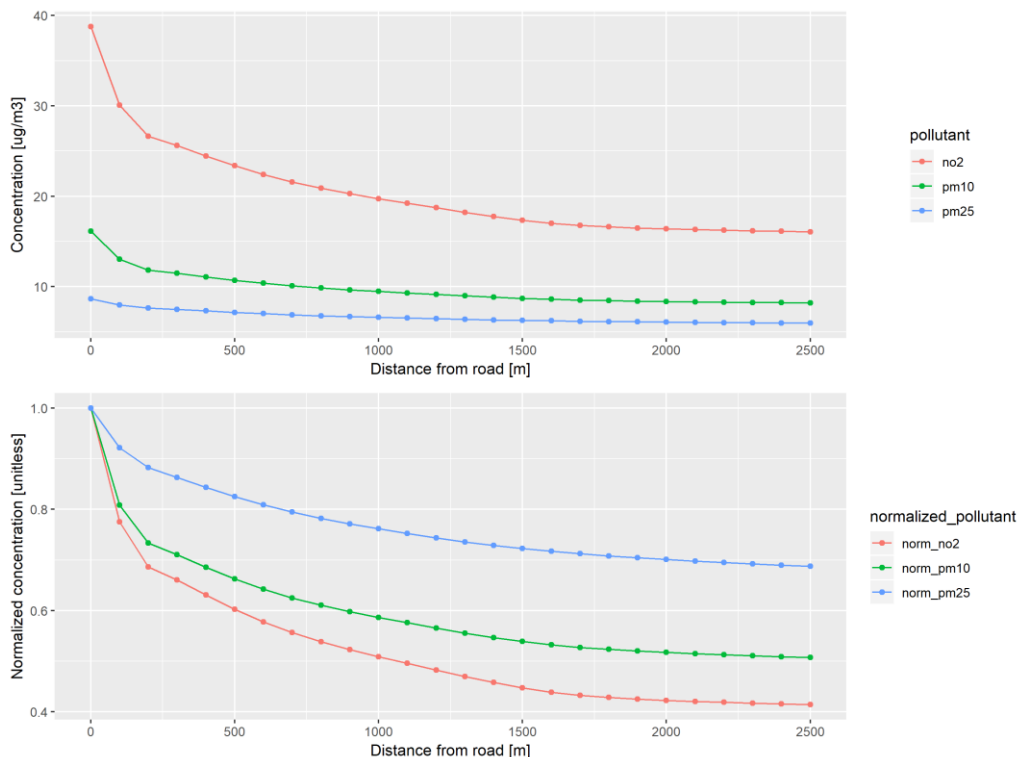


Figure A.9: Concentration levels of air pollutants NO₂ (red), PM₁₀ (green), and PM_{2.5} (blue) as a function of distance from road for absolute concentrations (top) and normalized concentrations (bottom). The data is derived from annual average concentration fields for the greater Oslo area as calculated by the EPISODE model (Slørdal et al., 2003).

It can be observed there that the spatial gradient of NO₂ and PM₁₀ are reasonably similar, whereas the horizontal spatial gradient for PM_{2.5} is significantly shallower, with the concentrations only decreasing to a level of around 70% of the on-road concentration at a distance of 2500 m. For the more traffic-related

pollutants of NO₂ and PM₁₀ we see reductions of 60% and 50% respectively. Compared to the urban/background ratios in urban areas based on measurement data (see Section 4.1.2 and 4.2.2), one can see that the modelled percentage reduction is somewhat overestimated, especially for PM₁₀.

The modelled spatial gradients are generally much weaker than those found by measurement campaigns that are reported in the literature and it should be noted here that such a simple extraction of spatial gradients from a long-term model average obviously cannot replace a comprehensive measurement campaign in any way.

A.4 Conclusions

A short literature study on the spatial gradients of air pollutants in the vicinity of roads was carried out and the preliminary results of a small modelling study with the EPISODE urban air quality model to extract typical spatial gradients was presented.

Overall, based on the literature review and the experiment with the EPISODE model, it seems to be an appropriate assumption that the horizontal spatial gradient as a function of distance from a major road is relatively similar for both NO₂ and PM₁₀, however the gradient of PM_{2.5} appears to be slightly less pronounced than for the other two pollutants. It is a fair assumption for the purposes of the ETC/ACM mapping tasks, which primarily only considers a distance of maximum 50-75 m from the road, that the horizontal spatial gradients for the three pollutants are relatively similar over such short distances.

References

Allen RW, Davies H, Cohen MA, Mallach G, Kaufman JD, Adar SD, 2009. The spatial relationship between traffic-generated air pollution and noise in 2 US cities. *Environ. Res.* 109, 334–342.

<https://doi.org/10.1016/j.envres.2008.12.006>

Beelen R, Hoek G, Vienneau D, Eeftens M, Dimakopoulou K, Pedeli X, Tsai M-Y, Künzli N, Schikowski T, Marcon A, Eriksen KT, Raaschou-Nielsen O, Stephanou E, Patelarou E, Lanki T, Yli-Tuomi T, Declercq C, Falq G, Stempfelet M, Birk M, Cyrus J, von Klot S, Nádor G, Varró MJ, Dédélé A, Gražulevičienė R, Mölter A, Lindley S, Madsen C, Cesaroni G, Ranzi A, Badaloni C, Hoffmann B, Nonnemacher M, Krämer U, Kuhlbusch T, Cirach M, de Nazelle A, Nieuwenhuijsen M, Bellander T, Korek M, Olsson D, Strömgren M, Dons E, Jerrett M, Fischer P, Wang M, Brunekreef B, de Hoogh K, 2013. Development of NO₂ and NO_x land use regression models for estimating air pollution exposure in 36 study areas in Europe – The ESCAPE project. *Atmos. Environ.* 72, 10–23. <https://doi.org/10.1016/j.atmosenv.2013.02.037>

Gilbert NL, Woodhouse S, Stieb DM, Brook JR, 2003. Ambient nitrogen dioxide and distance from a major highway. *Sci. Total Environ.* 312, 43–46. [https://doi.org/10.1016/S0048-9697\(03\)00228-6](https://doi.org/10.1016/S0048-9697(03)00228-6)

Gonzales M, Qualls C, Hudgens E, Neas L, 2005. Characterization of a spatial gradient of nitrogen dioxide across a United States-Mexico border city during winter. *Sci. Total Environ.* 337, 163–173.

<https://doi.org/10.1016/j.scitotenv.2004.07.010>

Hagler GSW, Baldauf RW, Thoma ED, Long TR, Snow RF, Kinsey JS, Oudejans L, Gullett BK, 2009. Ultrafine particles near a major roadway in Raleigh, North Carolina: Downwind attenuation and correlation with traffic-related pollutants. *Atmos. Environ.* 43, 1229–1234.

<https://doi.org/10.1016/j.atmosenv.2008.11.024>

Hitchins J, Morawska L, Wolff R, Gilbert D, 2000. Concentrations of submicrometre particles from vehicle emissions near a major road. *Atmos. Environ.* 34, 51–59. [http://doi.org/10.1016/S1352-2310\(99\)00304-0](http://doi.org/10.1016/S1352-2310(99)00304-0)

Horálek J, de Smet P, Schneider P, Maiheu B, de Leeuw F, Janssen S, Benešová N, Lefebvre W, 2018. Satellite data inclusion and kernel based potential improvements in NO₂ mapping, ETC/ACM Technical Paper 2017/14. Available at:

https://acm.eionet.europa.eu/reports/ETCACM_TP_2017_14_Improved_AQ_NO2mapping

Karner AA, Eisinger DS, Niemeier DEBA, 2010. Near-Roadway Air Quality : Synthesizing the Findings from Real-World Data 44, 5334–5344.

Massoli P, Fortner EC, Canagaratna MR, Williams LR, Zhang Q, Sun Y, Schwab JJ, Trimborn A, Onasch TB, Demerjian KL, Kolb CE, Worsnop DR, Jayne JT, 2012. Pollution gradients and chemical characterization of particulate matter from vehicular traffic near major roadways: Results from the 2009 queens college air quality study in NYC. *Aerosol Sci. Technol.* 46, 1201–1218.

<https://doi.org/10.1080/02786826.2012.701784>

McAdam K, Steer P, Perrotta K, 2011. Using continuous sampling to examine the distribution of traffic related air pollution in proximity to a major road. *Atmos. Environ.* 45, 2080–2086.

<https://doi.org/10.1016/j.atmosenv.2011.01.050>

Oftedal B, Walker SE, Gram F, McInnes H, Nafstad P, 2009. Modelling long-term averages of local ambient air pollution in Oslo, Norway: evaluation of nitrogen dioxide, PM₁₀ and PM_{2.5}. *Int. J. Environ. Pollut.* 36, 110–126. <https://doi.org/10.1504/IJEP.2009.021820>

Petersen WB, 1980. User's guide for HIWAY-2 - A highway air pollution model (No. EPA-600/8-80-018).

Pleijel H, Pihl Karlsson G, Binsell Gerdin E, 2004. On the logarithmic relationship between NO₂ concentration and the distance from a highroad. *Sci. Total Environ.* 332, 261–264.

<https://doi.org/10.1016/j.scitotenv.2004.03.020>

Schneider P, Castell N, Vogt M, Dauge FR, Lahoz WA, Bartonova A, 2017. Mapping urban air quality in near real-time using observations from low-cost sensors and model information. *Environ. Int.* 106, 234–247. <https://doi.org/10.1016/j.envint.2017.05.00>

Slørdal LH, Walker S-E, Solberg S, 2003. The Urban Air Dispersion Model EPISODE applied in AirQUIS 2003 - Technical Description (No. TR 12/2003), TR 12/2003. Kjeller, Norway.

European Topic Centre on Air Pollution
and Climate Change Mitigation

PO Box 1

3720 BA Bilthoven

The Netherlands

Tel.: +31 30 274 8562

Fax: +31 30 274 4433

Web: <http://acm.eionet.europa.eu>

Email: etcacm@rivm.nl

The European Topic Centre on Air Pollution and
Climate Change Mitigation (ETC/ACM) is a
consortium of European institutes under contract of
the European Environment Agency.

